Natural Hazards and Earth System Sciences (nhess)

Linking reported drought impacts with drought indices, water scarcity, and aridity: the case of Kenya

Marleen R. Lam[1], Alessia Matanó[2], Anne F. van Loon[2], Rhoda Odongo[2], Aklilu D. Teklesadik[3], Charles N. Wamucii[1], Marc J.C. van den Homberg[3], Shamton Waruru[4], and Adriaan J. Teuling[1]

[1]Hydrology and Quantitative Water Management (HWM), Wageningen University & Research (WUR), Wageningen, the Netherlands
[2]Institute for Environmental Studies (IVM), Vrije Universiteit Amsterdam, Amsterdam, the Netherlands
[3]510, an initiative of the Netherlands Red Cross, Anna van Saksenlaan 50, 2593 HT Den Haag, the Netherlands
[4]National Drought Management Authority (NDMA), Lonrho House, 8th Floor, Standard Street, P.O Box 10304, G.P.O. 00100 Nairobi, Kenya

Correspondence: Marleen R. Lam (marleen.lam@icloud.com), Adriaan J. Teuling (ryan.teuling@wur.nl)

Abstract.

The relation between drought severity ~~, as expressed through widely used drought indices,~~ and drought impacts is complex ~~. In particular in water-limited regions where water scarcity is prevalent, the attribution of drought impacts is difficult~~and so far relatively unexplored in the African continent. This study assesses the relation between reported drought impacts, drought indices, water scarcity, and aridity across several counties in Kenya. The monthly bulletins of the National Drought Management Authority in Kenya ~~have been used to gather~~ provided drought impact data. A Random Forest (RF) model was used to explore which set of drought indices (Standardized Precipitation Index, Standardized Precipitation Evapotranspiration Index, Standardized Soil Moisture Index and Standardized Streamflow Index) best explains drought impacts on ~~:~~ pasture, livestock deaths, milk production, crop losses, food insecurity, trekking distance for water, and malnutrition. The findings of this study suggest a relation between drought severity and the frequency of drought impacts, whereby the latter also showed a positive relation with aridity~~, whilst water scarcity did not~~. A relation between water scarcity and aridity was not found. The RF model revealed that every region, aggregated by aridity, had their own set of predictors for every impact category. Longer timescales (≥ 12 months) and the Standardized Streamflow Index were mostly present, indicating the importance of hydrological drought to predict drought impact occurrences. ~~The results of the RF model reveal that drought impacts can be explained by a range of drought indices across regions with different aridity.~~ While the findings strongly depend on the availability of drought impact data and the socio-economic circumstances within a region, this study highlights the potential of linking drought indices with text-based impact reports. In doing so, however, spatial differences in aridity and water scarcity conditions have to be taken into account.

1 Introduction

Drought events are among the world's most ~~impact-full~~ impactfull disasters (Stahl et al., 2016) and are receiving increasing attention across different scientific disciplines because of their complex links to both natural and socio-economic processes (Van Dijk et al., 2013; Van Loon et al., 2016a, b). Drought can be characterized as a slow-onset event whose impacts build up over time and extend spatially in relation to a range of contextual factors (Heinrich and Bailey, 2020). For instance, differences in societal and political characteristics can lead to a different range and magnitudes of impacts even though the intensity and duration of drought are similar (Savelli et al., 2022). At the same time, catchment characteristics also strongly influence the severity and propagation of drought events (Van Loon, 2015).

Although the multifaceted nature of drought drivers, drought detection and quantification usually rely primarily on the analysis of climatic and hydrological variables (Kchouk et al., 2022; Mishra and Singh, 2010; Yihdego et al., 2019). By expressing the anomaly with respect to the mean and variability of the local climate, drought characteristics can be compared across regions with different climate conditions. In addition, accumulation periods can be used to account for time lags and memory encountered in hydrological stores (Sutanto and Van Lanen, 2022). The most simple drought indices only use meteorological data while others include soil moisture or streamflow data (Yihdego et al., 2019). Meteorological and/or soil moisture (agricultural) drought are often expressed by the Standardized Precipitation Index (SPI), Standardized Precipitation Evapotranspiration Index (SPEI) and the Palmer Drought Severity Index (PDSI) (e.g., Baig et al. 2022; Kamruzzaman et al. 2022; Zhou et al. 2022) while the Standardized Streamflow Index (SSI), the Standardized Runoff Index and the Standardized Groundwater level Index (SGI) can be applied for hydrological drought (Van Loon, 2015). However, the analysis of hydro-meteorological variables alone may not be sufficient for the identification of the actual impacts of drought as the listed drought indices do not take into account the vulnerability of the system under analysis (Bachmair et al., 2015). To better evaluate and communicate about drought risk, it is necessary to establish reliable links between drought indices and impacts.

Due to the projected increase in drought ~~frequencies (Change, 2014), each successive drought event can result~~ frequency in some regions around the world (Seneviratne et al., 2021), the probability of successive drought events might rise, resulting in increased destabilization, ~~triggering~~ insecurity and resource-based ~~conflicts~~ conflict in contexts with high vulnerabilities (Peng et al., 2020). Monitoring and early warning (M&EW) is one important measure to enhance drought resilience. The goal of M&EW is to provide reliable and timely information on drought conditions (using a wide range of drought indices) to enable local society to better prepare and act accordingly (Wilhite et al., 2007). However, there is a gap between forecasting ~~a~~ an extreme hydro-meteorological event and the understanding of its potential impacts, as recognized by the World Meteorological Organization (WMO, 2015). ~~Linking drought impacts to drought indices can contribute to the ongoing development and improvements of the M&EW, aiming to reduce human and financial losses arising from a drought event.~~

~~Drought can occur in different parts of the terrestrial hydrological cycle. Therefore, droughts are generally classified as meteorological, hydrological, or soil moisture (agricultural) drought, which are related to, and influenced by, both natural processes and human activities (Van Loon, 2015; Van Loon et al., 2016b). Meteorological drought is typically defined only by the precipitation deficit, thereby not taking into account any actual conditions at or below the land surface. The precipitation~~

anomaly can then propagate through the hydrological cycle, resulting in soil moisture, streamflow and groundwater deficit
55 and hence, soil moisture and hydrological drought, respectively. Hydrological drought refers to anomalously low levels in
surface water (lakes, reservoirs, rivers) and/or groundwater. The detection and quantification of drought is usually done by
so-called standardized drought indices (Kchouk et al., 2022; Yihdego et al., 2019). By expressing the anomaly with respect to
the mean and variability of the local climate, drought characteristics can be compared across regions with different climate
conditions. In addition, accumulation periods can be used to account for time lags and memory encountered in hydrological
60 stores (Sutanto and Van Lanen, 2022). The most simple drought indices use only meteorological data while others include soil
moisture or streamflow data (Yihdego et al., 2019). Models using drought indices to forecast drought can detect climate signals
into soils and hydrology. Yet, the link between drought indices and socio-economic impacts has rarely been analyzed, in spite
of its importance for developing future measures to reduce vulnerability to drought.

The assessment and monitoring of drought impacts is complex given: (1) the great variety of drought impact categories;
65 (2) their possible propagation throughout the hydrological and social system; and (3) the difficulty of drought impact attribu-
tion. For Europe and the USA, drought impact databases have been developed, namely the European Drought Impact report
Inventory (EDII) (EDC, 2013) and the Drought Impact Reporter (NDMC, 2005)respectively. Some studies assessed the link
between drought impacts and drought indices, mainly with a focus on Europe. Unfortunately, such a structurally gathered
drought impact database does not exist for the Horn of Africa. Linking drought impacts to drought indices can contribute to
70 drought risk and vulnerability assessments which are useful for the development of drought monitoring and early warning
systems. These systems inform national and international organizations in providing timely and relevant assistance.

Several studies exist whereby drought impacts have been linked to drought indices. For instance, the qualitative dataset of
EDII has been used to assess the link between drought impacts and indices at continental (Blauhut et al., 2015), national (Stagge
et al., 2015), and regional scale (Bachmair et al., 2015, 2016, 2018). The results of multiple studies suggest that linking drought
75 indiceswith impacts is time, region, Linking indices to drought impacts has been done using several methods, such as logistic or
linear regression (Bachmair et al., 2018; Blauhut et al., 2015; Gudmundsson et al., 2014; Parsons et al., 2019; O'Connor et al., 2022; Stagge
, correlation analysis (Bachmair et al., 2016; Ma et al., 2020; Wang et al., 2020) and an ensemble regression tree approach (random
forest) (Bachmair et al., 2016, 2017; Wang et al., 2020). A multitude of drought indices, mostly SPI and SPEI with accumulation
periods ranging between 1 and sector specific (Bachmair et al., 2015, 2016, 2017; Blauhut et al., 2015; Ma et al., 2020; Stagge et al., 2015;
80 . This urges the need to study their relation in other setting such as 24 months, were linked to drought impact categories
applicable for the research area, for example wildfire activity (Gudmundsson et al., 2014) and agriculture (Parsons et al., 2019)
. However, according to our knowledge, there are no similar studies with a focus on the Horn of Africawhere drought impact
data has not been structurally gathered as compared to Europe and the US. Linking drought impacts with indices in that region
would generate new insights, because other types of drought impact categories are more applicable such as food insecurity,
85 livestock hunger/death/migration, diseases, and conflict (Quandt, 2021).

Linking drought impacts with drought indices is regarded as difficult as there is often no strong intuitive cut-off within impact
categories between non-drought and drought conditions (Hall and Leng, 2019). For instance, water scarcity conditions can be
the result of anthropogenic actions and can lead to the same impacts experienced as during drought conditions (Van Loon and

Van Lanen, 2013). Water scarcity is a frequent phenomenon within (semi)-arid regions (Maliva and Missimer, 2012) and it occurs when water demand (both societal and ecological water demand) exceeds water supply (Kimwatu et al., 2021). It often leads to long-term unsustainable use of water resources (Van Loon and Van Lanen, 2013). Whereas aridity, based on the ratio of long-term annual precipitation and potential evapotranspiration rates (UNESCO, 1979), is regarded as a relatively constant value, water scarcity is dynamic in time and related to both decreases in water availability and increases in water demand. The simultaneous presence of both water scarcity (partly driven by anthropogenic causes) and meteorological drought in an arid region can lead to a difficult attribution of the impacts experienced. However, separation of the causes of impacts is needed to generate reliable information to stimulate early action in the affected sectors during drought events.

In this study, we focus on Kenya. Strong gradients characterize the country in precipitation, aridity, water yield (i.e., amount of precipitation minus total actual evapotranspiration), and water scarcity (Mulwa et al., 2021; Wamucii et al., 2021), in combination with the availability of reported impacts of recent droughts. The country has experienced several drought events in the recent past: for instance, 2008–2011 was classified as a prolonged severe drought (Mutsotso et al., 2018) and the drought in 2016–2017 was considered a national disaster (Kew et al., 2021; Ondiko and Karanja, 2021), with more than three million people under food insecurity (Thomas et al., 2020). The country has also experienced a diverse range of drought impacts such as cattle mortality, wildlife death, famine, human losses, and severe food shortages (Ondiko and Karanja, 2021). The presence of drought hazards, drought impacts, water scarcity, and aridity makes this country a suitable study area to analyse their relations. In this context, the following main research question is formulated: What is the relation of drought impacts with drought indices and with water scarcity under different aridity levels?

It is expected that drought events and impact occurrences vary between climate zones. We hypothesize that drought impacts (and therefore the relationship between drought indices and impacts) will differ across regions with different aridity characteristics in Kenya because of the distinct socio-economic settings, possibly making arid areas more vulnerable than more humid areas (Maliva and Missimer, 2012). Furthermore, it is expected that water scarcity will show a relation with aridity due to the presence of unreliable water conditions.

2 Data and methods

2.1 Study area

Kenya is situated in East Africa. Its highest altitudes can be found in the central highlands (with the highest peak of over 5000 m above sea level observed in Mt. Kenya forested water tower), and low-lying regions can be found in the East, Northwest, and Northeast. The country mostly has an arid and semi-arid climate which comprises about 80% of the territory and hosts about one-quarter of the population (FEWS NET, 2013) of approximately 53 million people (The World Bank, 2020). Mean annual rainfall is less than 250 mm in the semi-arid and arid areas and more than 2.000 mm in the mountainous areas. Long rains are experienced from March to May (MAM) while short rains occur from

October to December (OND) (Ayugi et al., 2020). The medium to high potential agricultural areas are in the highland areas in the central and western parts of the country (sub-humid/humid zones) where the population density is six times the country's average. Farming is the primary livelihood (both subsistence as well as commercial) for more than 75% of the population. Less
125 than 4% are pastoralists who mainly live in the semi-arid and arid regions which are characterized by poorly distributed and unreliable rainfall (FEWS NET, 2013).

For this study, six counties have been selected according to different aridity levels, livelihood zones, and available drought impact information. Figure 1 presents the counties considered in this study (Fig.~~1a.~~ 1a), the aridity (Fig.1b), and the livelihood zones (Fig.~~1c.~~ 1c). Marsabit is an arid county (arid index 0.03–0.20) in the Northern pastoral zone while Baringo, Kitui and
130 Kwale are considered semi-arid (arid index 0.20–0.50). Baringo is located in the western part of Kenya and encompasses mostly a ~~high potential~~ high-potential agricultural zone while Kitui and Kwale are both mostly marginal mixed farming zones. Nyeri is situated in the central highlands and encompasses mostly a ~~high potential~~ high-potential agricultural zone. ~~However,~~
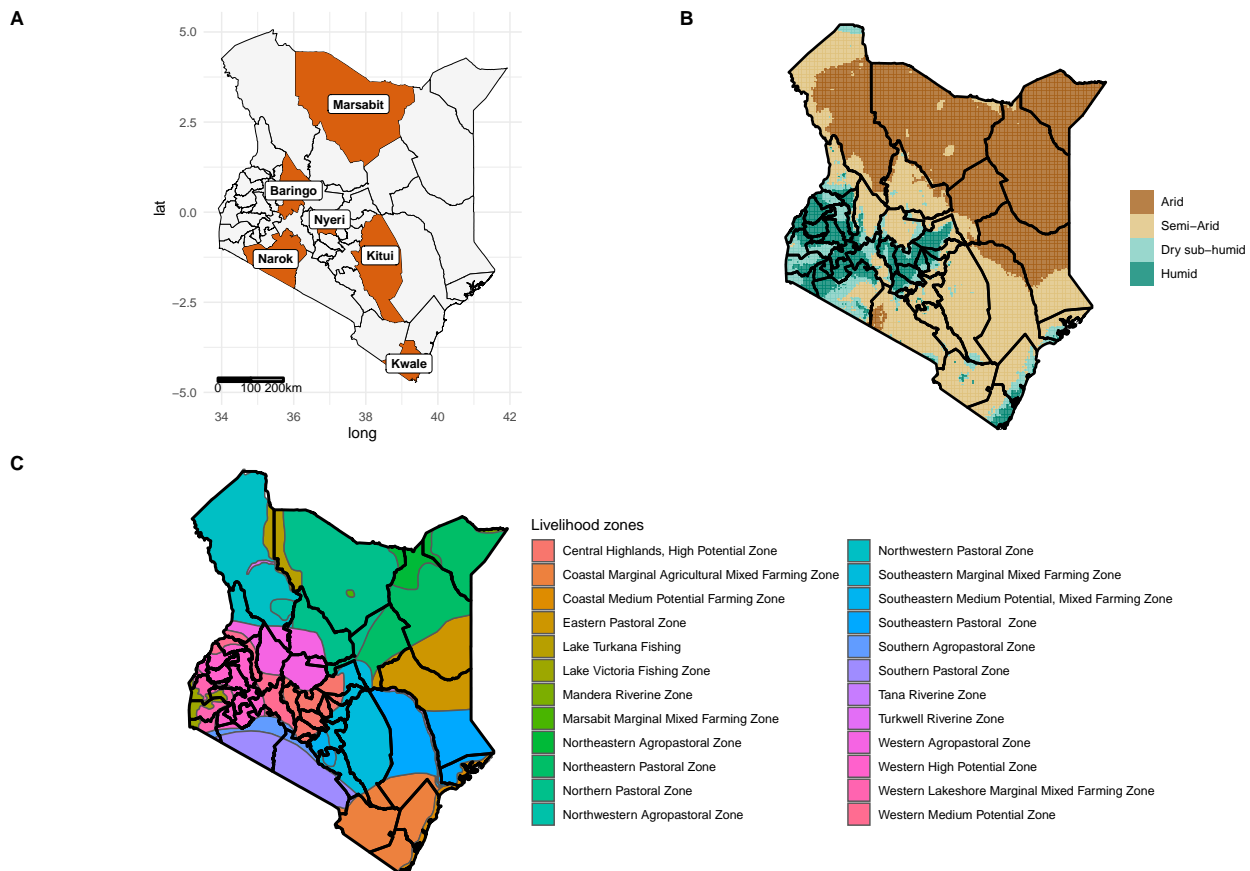
Figure 1. Study area and its main characteristics. a) Counties considered in this study, b) distribution of aridity, and c) distribution of livelihood zones.

~~this study will specifically focus on a region in Nyeri~~This study specifically focuses on one district in the Nyeri county, namely Kieni~whereby the main livelihood~, according to the availability of drought impact data provided by the National Drought Management Authority (NDMA). From now on, with Nyeri, we only refer to the Kieni district. The main livelihood in Kieni is connected to agropastoral activities (FEWS NET, 2013). Narok mostly consists of (agro)pastoral grounds. Both Nyeri and Narok are regarded sub-humid zone regions (arid index 0.50–0.75).

2.2 Data

To study the linkage between drought impacts, drought indices, water scarcity, and aridity, several datasets were used. In this study, we used ~~re-analysis~~ reanalysis data to analyse several hydro-meteorological variables (Section 2.2.1), national drought bulletins for ~~extracting~~ text-based drought impact data (Section 2.2.2), and a gridded water scarcity dataset from McNally et al. (2019) (Section 2.2.3).

2.2.1 Hydro-meteorological and soil moisture datasets

Precipitation data

Precipitation data ~~has been~~ is retrieved from the Multi-Source Weighted-Ensemble Precipitation (MSWEP ~~) version 1.1~~v2) (Beck et al., 2019). This is a global gridded precipitation (P) dataset that takes full advantage of the complementary nature of the highest quality gauge-, satellite- and reanalysis-based P estimates, available as a function of timescale and location, by optimally combining them ~~(Beck et al., 2017a)~~(Beck et al., 2019). MSWEP covers the period ~~1979–present~~ 1979-2020 at 3 hourly temporal and 0.1 degree spatial resolution. This dataset ~~was~~ is chosen for this analysis based on its spatial and temporal resolution, good performance in capturing spatial and temporal variation of drought conditions (Xu et al., 2019) and also for consistency purposes.

Soil moisture and Potential Evapotranspiration data

The Global Land Evaporation Amsterdam Model (GLEAM) version 3.5a ~~(v3.5a)~~ consists of a set of algorithms dedicated to the estimation of land surface evaporation (also referred to as evapotranspiration) and root zone soil moisture from satellite and reanalysis data at the global scale and 0.25 degree spatial resolution (Martens et al., 2017; Miralles et al., 2011). The model uses the ~~latest version of MSWEP precipitation, (v2.8), European Space Agency Climate Change Initiative (ESA-CCI) soil moisture(v5.3), and~~ MSWEP dataset (Beck et al., 2017a), satellite-observed soil moisture, reanalyis air temperature and radiation, and Vegetation optical depth (VOD) (Liu et al., 2011) to produce terrestrial evaporation and root-zone soil moisture (Martens et al., 2017). The ~~model uses~~ GLEAM model applies the Priestley and Taylor ~~equation~~ (PT) equation (Priestley and Taylor, 1972) to calculate the Potential Evapotranspiration (PET) based on observations of ~~ERA5~~ European Centre for Medium-Range Weather Forecasts (ECMWF), ERA-Interim surface net radiation and near surface air temperature (Dee et al., 2011). GLEAM datasets have been used in multiple hydro-meteorological applications and recent drought conditions studies in the Horn of Africa ~~(Javadinejad et al., 2019; Nicolai-Shaw et al., 2017; Peng et al., 2020)~~(e.g., Javadinejad et al. 2019; Nicolai-Shaw et al. 2017; Peng). For this study, the GLEAM potential evaporation (PET) and root zone soil moisture ~~were used (see http://www.gleam.eu)~~ data (see http://www.gleam.eu) is used for the period 2010–2020.

Streamflow data

Streamflow data ~~has been~~ is retrieved from the Global Flood Awareness System (~~GLOFAS~~GLoFAS) which consists of global gridded reanalysis river discharge data, with a horizontal resolution of 0.1 degree at a daily time step and time period of 1979–present (Harrigan et al., 2020). It combines ~~surface and sub-surface runoff from the HTESSEL~~ the land surface model ~~used within ECMWF 's global atmospheric reanalysis (ERA5) with the LISFLOOD hydrological and~~ runoff component of the ECMWF ERA5 global reanalysis (Balsamo et al., 2009; Hersbach et al., 2020) with a hydrological rainfall-runoff channel routing model ~~(Harrigan et al., 2020). LISFLOOD calculates a water balance at a six hourly or daily temporal resolution with 0.05 degree spatial resolution (see http://www.globalfloods.eu/).~~ (Van Der Knijff et al., 2010; Hirpa et al., 2018) (see http://www.globalfloods.eu/). The GLoFAS dataset was chosen because of limited river discharge observational data in the study area.

2.2.2 ~~The~~ Impact data from the National Drought Management Authority (NDMA)

The monthly ~~written bulletins containing drought impact data in Kenya were retrieved from~~ county early warning bulletins of the National Drought Management Authority (NDMA) of Kenya were used to retrieve drought impact data. The NDMA has offices in the 23 Arid and Semi-Arid Lands (ASALs) of Kenya which are considered vulnerable to drought. The Authority performs sentinel surveillance each month based on rainfall ~~amounts~~estimates from the Tropical Application of Meteorology Using Satellite Data and Ground-Based Observations (TAMSAT) (Maidment et al., 2014; Tarnavsky et al., 2014), vegetation and water status. ~~In addition, food~~ Food security threats are assessed on (1) Availability aspects: cropping area and yield (maize, beans, sorghum etc.), animal body condition, milk production, livestock death, and forage condition; (2) Access factors: market access and performance, food availability in the household and market. This data is fed into a web-based software created by the Kenya's Drought Early Warning System and sent directly to the county director. The director analyzes the data against the three-monthly Vegetation Condition Index (~~VCI) (provided to them in the form of charts and graphs) where after he computes the Food Consumption index and~~ VCI-3 month) provided at county level and on a monthly basis. The VCI is obtained from an advanced filtering method for Moderate Resolution Imaging Spectroradiometer (MODIS) normalized difference vegetation index (NDVI) at pixel level developed and implemented by the University of Natural Resources and Life Sciences (BOKU) (Klisch and Atzberger, 2016). The MODIS NDVI data undergoes offline smoothening based on the Whittaker smoother (Atzberger and Eilers, 2011) to daily NDVI values, and near real time filtering based on available observations

Table 1. Falkenmark index for the water scarcity level.

Category	m^3/year /capita
heightNo stress	>1700
Stress	1000–1700
Scarcity	500–1000
Absolute scarcity	<500

within the past 175 days (Atzberger et al., 2014). In addition, the director calculates the percentage of children under five years with malnutrition using the Mid-Upper-Arm Circumference (MUAC) color codes of the United Nations Children's Fund (UNICEF) against the long term average. Lastly, the Food Consumption Score (FCS) is computed based on food frequency and diversity based on a seven-day recall of food consumed at the household level, taking into account the relative nutrition importance of different food groups (WFP, 2008). A poor FCS means a lack of vegetable consumption every day and low consumption of protein rich food such as dairy and meat.

2.2.3 Water scarcity

This study has utilized water scarcity (WS) data from McNally et al. (2019). The data is a monthly water scarcity dataset with a spatial resolution of 0.1 degree for Africa from March 2018 to the present. The water scarcity dataset is based on hydrological data from the Famine Early Warning System Network (FEWS NET) Land Data Assimilation System (FLDAS) and gridded population data from WorldPop (2015). The FLDAS's Noah 3.6 land surface model is derived from the Climate Hazards Group InfraRed Precipitation with Station (CHIRPS) rainfall and NASA's Modern-Era Retrospective analysis for Research and Applications (MERRA-2) meteorological forcing. The different classes of water scarcity are defined by the Falkenmark index (Falkenmark et al., 1989). This index categorises the amount of renewable freshwater available for each person per year, as shown in Table 1. The water scarcity dataset of McNally et al. (2019) provides monthly water scarcity data despite the yearly values of the Falkenmark index. For this, McNally et al. (2019) used the yearly values of the Falkenmark index to classify the water scarcity on a monthly basis by using a 12-month running total of the streamflow data. The water scarcity dataset was aggregated for the whole of Kenya whereafter monthly average values per county have been calculated and classified by the Falkenmark index. More information about the water scarcity dataset can be found in Appendix A.

2.3 Methods

2.3.1 Drought indices

There are several widely-used standardized drought indices to characterize meteorological, hydrological and soil moisture drought. The Standardized Precipitation Index (SPI), devised by McKee et al. (1993), allows quantification of precipitation deficits/ surpluses on a range of different accumulation periods. The SPI is calculated by summing daily MSWEP precipitation over n months (termed accumulation periods) obtaining a monthly temporal resolution. Monthly precipitation values are then ranked and their percentiles calculated. The number of zeros is taken into consideration following recommendations from Stagge et al. (2015). Thereafter, the values are standardized to a normal distribution with values between -3 and 3 by ranking, so without fitting a parametric statistical distribution (as tested by Stagge et al. 2015, and others). This is justifiable in our case because the distribution is already approximately normal. When we compared the SPI calculated with a statistical distribution and SPI with ranking, the results were similar. Finally, the gridded SPI values are spatially aggregated to county resolution by averaging the

SPI values of all grid ~~cell~~ cells per county, to match the spatial resolution of the recorded impacts. Negative values of the drought indices indicate dryer than average conditions while positive values indicate wetter than average conditions. An area is considered in drought when the drought index is below 0. A similar procedure ~~was~~ is used in the calculation of the indices mentioned below.

The Standardized Precipitation Evapotranspiration Index (SPEI) is similar to SPI ~~but also incorporates temperature by including evaporation anomalies (Vicente-Serrano et al., 2010). SPEI is calculated from~~ (Vicente-Serrano et al., 2010), but instead of precipitation it uses the difference between precipitation and potential evapotranspiration as input (Beguería et al., 2014). Thus, it provides a water balance and does not have the zero precipitation problems encountered by SPI. SPEI incorporates the effects of potential evapotranspiration, which depends strongly on the temperature. The Standardized Soil Moisture Index (SSMI) is based on mean monthly GLEAM ~~rootzone~~ root-zone soil moisture content. Finally, the Standardized Streamflow Index (SSI) is based on mean monthly GloFAS discharge values (Nalbantis, 2008). A mask ~~was~~ is created with mean monthly discharge values above 1 m^3/s. This mask ~~was~~ is then used for the calculation of the SSI. SSI and SSMI are often used to take into account drought propagation through the hydrological cycle and are therefore able to better represent catchment memory compared to SPI and SPEI.

All the four drought indices (SPI, SPEI, SSMI and SSI) ~~were~~ are calculated on a monthly timescale at the original grid scale with an accumulation period of 1, 3, 6, 12 and 24 months. The drought indices ~~were~~ are calculated for the period 1980–2020. However, for investigating drought indices-impact relationships, we ~~used~~ use drought indices between ~~2014–2020~~July 2013 and 2020, in accordance with the availability of drought impact data. In this study, SPI and SPEI represents meteorological drought, as they are based on precipitation and evapotranspiration anomalies. SSMI represents soil moisture drought, while SSI represents hydrological drought, as they are based on soil moisture and streamflow anomalies respectively (Yihdego et al., 2019). We also used SPI and SPEI with longer accumulation periods as a proxy for soil moisture and hydrological drought (Dai et al., 2020; Senev.

2.3.2 Drought impact data

This research gathered drought impact data from the National Drought Management Authority (NDMA) for the ~~above specified~~ above-specified counties in Kenya, ~~between 2014 and 2020.~~ from July 2013 to December 2020 (https://www.ndma.go.ke/). The NDMA was established by the Kenyan government in 2016 with the aim to set up and operate early warning drought systems and to develop drought preparedness strategies and contingency plans (Barrett et al., 2020). Their website provides monthly county early warning bulletins assessing food security in 23 regions using socio-economic and biophysical factors. These text-based impact reports provide the input for the impact categories considered in this study. The impact categories are based on the available information from the NDMA and can therefore be regarded as categories of socio-economic relevance for Kenya.

The heading of the early warning bulletins provides information on the drought phase classification, according to the following levels: 'normal', 'alert', 'alarm', 'emergency' or 'recovery'. This classification is based on biophysical variables, such as SPI and VCI, and socio-economic indicators of food security (Mwangi et al., 2022). Only the bulletins mentioning the phases 'alert', 'alarm' or 'emergency' were considered for this analysis. Furthermore, the early warning bulletins inform

about the severity of drought by categorizing the state of the monitored biophysical and socio-economic indicators. This categorization is in general related to the following five levels: very good, normal, moderate, severe, or extreme conditions.

260 We converted this information into binary data by assigning a value of 0 to very good and normal conditions and a value of 1 to moderate, severe, and extreme conditions. This study defines a drought impact as a negative or adverse effect on economic, environmental or social level which are experienced under drought conditions (Erian et al., 2021). The ~~text-based impact data were turned into quantitative binary values by looking if the drought impact category value was different from the normal values for that time of the year (compared to previous years).~~ following impact categories were considered:

265 – Pasture (i.e. livestock migration pattern, quality and quantity of pasture, livestock body condition);

   – Livestock deaths;

   – Milk production;

   – Food insecurity (based on the Food Consumption Score, FCS);

   – Crop losses;

270 – Trekking distance to gather water for households;

   – Malnutrition.

~~Jaccard similarity~~ The Jaccard similarity coefficient for binary values, first developed by Paul Jaccard in 1901 (Jaccard, 1912), was used to measure the similarities between the occurrence of drought impact categories (Niwattanakul et al., 2013). It measures the size of intersection of the two binary sets divided by the size of the union, the following equation is given:

275
$$Jaccard(A, B) = \frac{|A \cap B|}{|A \cup B|} \tag{1}$$

2.3.3   Random Forest Modelling

A machine learning algorithm, namely the classification type of Random Forest (RF), ~~have~~ has been used to assess the ~~relation between the drought impact categories and drought indices (Rpackage randomForest, version 4.6-14). It is a~~ drought indices best linked to drought impacts per region with the same aridity level. RF is a powerful tool for developing a predictive
280 model and is a fairly new technique for linking drought indices with impacts but showed high potential in the studies of ~~(Bachmair et al., 2016, 2017)~~ Bachmair et al. (2016, 2017). The RF algorithm, proposed by Breiman (2001), ~~combines several randomized decision trees and aggregates their predictions~~ constructs multiple random independent decision trees as an ensemble to reduce the risk of overfitting (this study used 1000 trees). Each tree is constructed on boot-strapped fixed size sub-samples of the data and predictions are made by averaging. ~~It is designed to minimize the overall classification~~ Approximately
285 two-third of the training dataset is used for building a tree while one third is not used, called the out-of-bag (OOB) data.

This generates an additional estimate of performance, namely the OOB error which is ~~irrespective of the class distribution (Elreedy and Atiya, 2019). Therefore, the datasets with amount of drought impacts per impact category and the corresponding drought indices was balanced by using a synthetic minority oversampling technique (SMOTE) and randomized under-sampling (RUS). The min-max method was used as a normalization technique to scale the datasets.~~ a method to measure the prediction error of the random forest. The predictor variables are the drought indices as mentioned in section 2.3.1, and the response variables are the binary time series of reported drought impacts derived from the monthly early warning bulletins of the NDMA.

The drought impact datasets were ~~aggregated by aridity~~ clustered according to aridity levels: Marsabit (arid), Baringo, Kwale and Kitui (semi-arid) and Narok/Nyeri (sub-humid). ~~We developed a random forest model for each of the drought impact categories aggregated per county with the same degree of aridity. Model performance was evaluated using a subset (25%) of the original dataset as test~~ For each of these regions, a RF model was constructed per drought impact category. In order to validate the model, a training and test dataset were constructed with a proportion of 75% and 25% of the original dataset. The training datasets were balanced using a synthetic minority oversampling technique (SMOTE) and randomized under-sampling (RUS) as the RF algorithm is sensitive to class imbalances. The caret package in Rstudio (version 6.0–93) was used to conduct the RF model analyses, after Kuhn (2008). The 'variable importance' function (varImp) of this package was used to determine the importance of a predictor variable for the model to make accurate predictions. Specifically, the prediction accuracy on the OOB data is recorded for each tree, which is also done after permuting each predictor variable. The difference in accuracy between the two models is then averaged over all trees, and normalized by the standard error (Kuhn, 2008; Liaw et al., 2002).

The predictive power of the RF models was assessed in two ways. First, the overall model performance on the test set was evaluated based on a 10-fold cross-validation. Therefore, for each model run, the test dataset was split into 90% for training and 10% for prediction. This allows the evaluation of the performance of the RF model on unseen data excluded from model fitting. As model performance metrics, we computed the OOB error rate and the accuracy. Second, the RF model was fitted to the test dataset to see how the model would perform on unseen and unbalanced data. The ~~area~~ following model performance metrics were used to see how the RF model performed on the test set; precision, recall, the F1-score, and the "Area under the ROC ~~(Receiver Operating Characteristic) curve~~curve" (AUC) ~~describes the model's ability~~ (Hanley and McNeil, 1982). Precision is the true impacts divided by anything that we predicted as impact while recall is the true impacts divided by anything that should have been predicted as an impact. The F1-score is a combination of recall and precision. The AUC describes whether the model was able to predict the occurrence and non-occurrence of ~~events correctly. A more detailed explanation about the RF model and the tuning of parameters can be found in~~ impacts correctly. We validated the results of the RF model by conducting a point-biserial correlation. This method measures the direction and strength of a relationship between a continuous and categorical variable (Essen and Akpan, 2018). The results of this analysis will not be discussed in detail but are included in Appendix C.

Table 2. Total amount of reported drought impacts between 2016 and 2020 and the share of drought impact categories (%) for each county.

County	Baringo	Kitui	Kwale	Marsabit	Narok	Nyeri
~~Count~~ Number of impacts	45	93	50	124	51	44
Pasture (%)	17.8	30.1	28.0	20.2	25.5	29.6
Livestock deaths (%)	11.1	5.4	6.0	9.7	9.8	4.6
Milk production (%)	22.2	22.6	26.0	18.6	27.5	31.8
Food insecurity (%)	4.4	10.8	10.0	15.3	3.9	15.9
Crop losses (%)	6.7	1.1	4.0	2.4	2.0	2.3
Trekking distance water (%)	20.0	15.1	12.0	16.9	17.7	9.1
Malnutrition (%)	17.8	15.0	14.0	16.9	13.7	6.8

3 Results

3.1 Drought indices and drought impacts

320 To ~~visually represent the relationships~~ illustrate the relationship between drought impacts and drought indices, a timeframe from 2016 to 2020 is ~~constructed to include the drought of 2016/2017. Most drought impacts were reported in Marsabit and Kitui while Baringo and Nyeri reported the lowest amount of impacts (Table 2)~~chosen. Table 2 presents the share of each drought impact category (in %) with respect to the total number of drought impacts per county. Most drought impacts were reported in Marsabit and Kitui while Baringo and Nyeri reported the lowest amount of impacts. Pasture and Milk production

325 are the most reported drought impacts across the counties, with values between 17.8 and 31.8%. Noticeable is that Nyeri has the highest share in pasture-related impacts: Pasture impacts are 29.6% and Milk production impacts are 31.8% of the total impacts for Nyeri. The least reported drought impacts are on Crop losses, Livestock deaths and Food insecurity with average values of 3.1%, 7.8% and 10.1% respectively. Impacts related to Malnutrition are the highest in Baringo (17.8%) and Marsabit (16.9%), while Nyeri has by far the lowest amount of Malnutrition impacts (6.8%). Baringo has the highest share of impacts

330 concerning Trekking distance for water (20.0%) while Nyeri has the lowest percentage (9.1%).

~~The least reported drought impacts are on Crop losses, Livestock deaths and Food insecurity with average values of 3.1%, 7.8% and 10.1% respectively. Impacts related to Malnutrition are the highest in Baringo (17.8%) and Marsabit (16.9%), while Nyeri has by far the lowest amount of Malnutrition impacts (6.8%). Baringo has the highest share of impacts concerning Trekking distance for water (20.0%) while Nyeri has the lowest percentage (9.1%).~~

335 A ~~timeline~~ time series of the drought indicator SPEI for different accumulation periods (1, 3, 6, 12 and 24 months) and a timeline with drought impacts are presented for Marsabit and Nyeri in Figures 2a and 2b for the time period 2016–2020. We choose to visualize the drought impacts and SPEI time series of those counties because of their contrasting aridity levels. Similar figures for the other counties are included in the Supplement (Figures S1-S4). Noticeable is that Marsabit experienced more extreme drought (in frequency and intensity) than Nyeri: SPEI-03 with a value of -2.22 in November 2018 was the most

340 extreme drought for Marsabit while SPEI-12 with a value of -1.90 in April 2017 was the most extreme drought for Nyeri.

SPEI-24 indicates that Marsabit experienced a multiyear drought from January 2016 to May 2019. The drought of 2016–2017 is well visible for both counties. In addition, there was a drought at the end of 2018 and 2019 which is more pronounced for Marsabit than for Nyeri. Regarding the drought impacts, Marsabit reported drought impacts (N = 124) from March 2016 until December 2020 with the exception of the periods between March and December 2018 and between November 2019 and August 2020. Nyeri reported drought impacts (N = 44) from February 2017 until September 2019 with only one impact reported between November 2017 and January 2019.

Taking the 2016/2017 drought as an example, the drought impacts reported in Marsabit are between March 2016 and February 2018 and highly overlap with SPEI-12 values lower than 0, which is prevalent between April 2016 and March 2018. Reported drought impacts for Nyeri are between February 2017 and March 2017 and correspond most with SPEI-12 values lower than 0, occurring from October 2016 until April 2018. A direct relationship with the In general, drought impact occurrence does not happen simultaneously with the drought time period of the other accumulation periods is not directly visible, except for SPEI-24. In particular, most of the analysed drought impacts occur after the onset of drought identified with accumulation periods of less than 12.
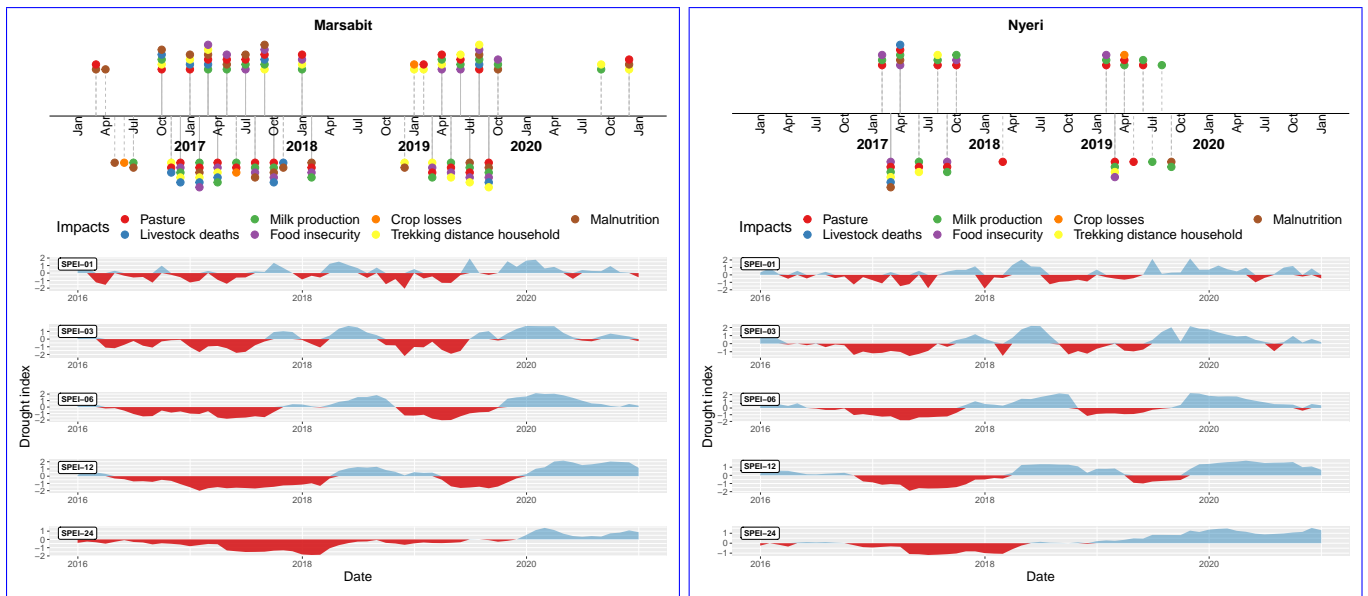
(a) Marsabit (b) Nyeri

Figure 2. A timeline time series of the drought indicator index SPEI for different accumulation periods (1, 3, 6, 12 and 24 months) and a timeline with drought impacts for Marsabit (arid) and Nyeri (sub-humid). The colored dots indicate the type of impact occurrence. Negative values of SPEI indicate dryer than normal periods (indicating a drought) are presented in red) while positive values are indicate wetter than normal (blue).

Table 3. Correlation between the impact categories (Jaccard similarity): the asterisks indicate the statistical significance (p value < 0.05) in accordance with Chung et al. (2019).

Impact category	Pasture	Livestock deaths	Food insecurity	Milk production	Trekking distance water	Malnutrition
Livestock deaths	0.23*					
Food insecurity	0.39*	0.27*				
Milk production	0.63*	0.23*	0.42*			
Trekking distance water	0.50*	0.26*	0.29	0.47*		
Malnutrition	0.41	0.20	0.27	0.34	0.34	
Crop losses	0.15	0.04	0.00*	0.11	0.11	0.11

(a) Water scarcity over March 2018 and 2020.   (b) Water scarcity and drought impacts.
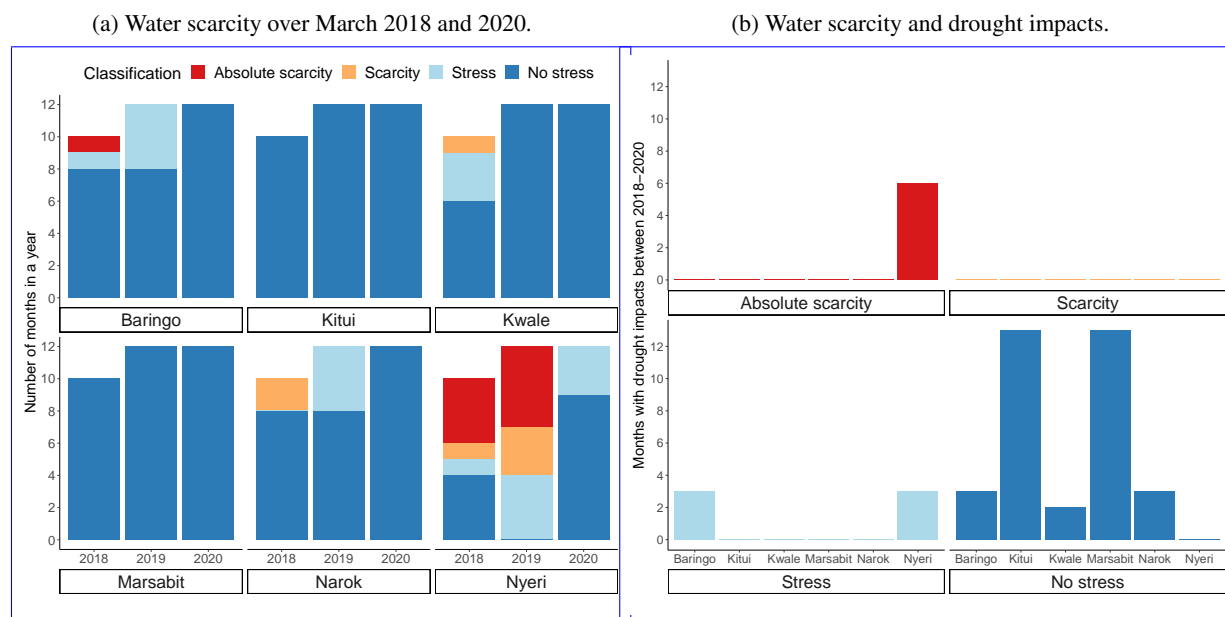
Figure 3. The degree of water scarcity per year (March 2018–2020) across the counties (a) and months with drought impacts in relation to water scarcity (b) (McNally et al., 2019).

In this study, we We also explored the relation between reported drought impacts (Table 3) by using the Jaccard similarity

355   for binary values. The results are shown in Table 3 whereby closer to 1 means that the datasets are more similar to each other than closer to 0. Pasture and Milk production are a bit related (have the highest significant Jaccard similarity of 0.63) while Crop losses are not much related to any other impact category (<0.20). Trekking distance to water points indicates a bit of relation with Pasture (0.50) and Milk production (have a significant Jaccard similarity of 0.50 with Pasture and 0.47)with Milk production. Other relations between impact categories are not very prevalent (<have a Jaccard similarity below 0.40).

3.2 Drought impacts and water scarcity

The degree of water scarcity per year (in number of months) across the counties is visualized in Figure 3a. This is done from March 2018 due to the length of the WS dataset. Kitui and Marsabit experienced no water stress since March 2018 ~~(start of timeframe WS dataset)~~ while Nyeri experienced stress, scarcity and absolute scarcity during six out of ten months in 2018 and all months of 2019. Baringo, Kwale and Narok did also experience stress and scarcity conditions (respectively 2, 4 and 2 months out of 10 for 2018 ~~(WS dataset starts at March 2018)~~ and 4, 0 and 4 months out of 12 for 2019) but with a lower frequency than Nyeri.

Figure 3b shows the amount of months with drought impacts during 2018 and 2020 in relation to the degree of water scarcity. Nyeri experienced 9 months with drought impacts between March 2018 and 2020, of which 6 months with absolute water scarcity and 3 months in a stress situation. Kitui and Marsabit experienced 14 months with drought impacts but did not experience any degree of water scarcity. Baringo had 6 months with drought impacts, of which half of the months were showing stress situations.

3.3 ~~The~~ Random Forest ~~model~~ to link drought impacts and drought indices

The performance of the Random forest (RF) models per impact category is shown in Table 4. The ~~AUC~~ regions are aggregated by their aridity levels: Marsabit is classified as arid, Baringo/Kitui/Kwale are semi-arid and Narok/Nyeri are sub-humid regions. The RF models have been trained on 75% of the data and tested on 25% of the data. The performance of the RF model has been evaluated by looking at the OOB and accuracy while precision, recall, the F1-score and the AUC are used as performance metrics for the test data set.

The AUC values as performance metric for the test data set ranges from 0.50 to 1.00. The performance of the models for the drought impacts on Pasture~~and Livestock have the~~, Livestock and Milk production for the arid and sub-humid regions had the best fit, with AUC values ranging from ~~0.87~~ 0.76 to 1.00. Models developed for the drought impact of Malnutrition ~~have had~~ the worst fit, with all AUC values below 0.60. ~~The models for the arid region of Marsabit (MA) and the~~ In general, the models related to the arid and sub-humid regions ~~of Narok and Nyeri (NA, NY) had the best overall fit with diverse ranges of performance among the impact categories. For instance, the model on Marsabit concerning Food insecurity has~~ performed better than the models of the semi-arid region with an exception of the model developed for Crop losses (AUC of 0.75). Noticeable is that the model of the arid region in relation to Food insecurity had very high performance ~~(~~values (F1-score of 1.00 ~~) while the one in Narok/Nyeri has a low performance (0.53). For Marsabit and Narok/Nyeri (arid and~~ and AUC of 1.00) which is as well the case for the sub-humid ~~regions respectively) , the models related to activities of pasture (Pasture, Livestock deaths and Milk production) have very high performance rates (AUC > 0.87).~~ regions in relation to Trekking distance of water for households (F1-score of 0.75 and AUC of 0.92). We will only discuss the variable importance metrics of the RF models (1) that performed relatively well on the test dataset because it is important that the model can predict drought impacts based on unseen data (not used for model training) and (2) whereby the results were similar with the results of the point-biserial correlation (Appendix C). The last column of Table 4 indicates if the model is discussed in terms of variable importance.

Table 4. ~~Performance~~ RF performance metrics: the performance of the RF model ~~per impact category~~ is tested by looking at the OOB and ~~arid characteristics (MA = Marsabit~~ the accuracy while precision, ~~BA = Baringo~~ recall, ~~KI = Kitui, KW = Kwale, NA = Narok~~ the F1-score and ~~NY = Nyeri~~ the AUC are computed as performance metrics for the performance of the RF model on the test data set (25%).

Aridity level	Impact category	OOB	Accuracy	Precision	Recall	F1
Arid	Pasture	14.81	0.87	0.89	0.89	0.89
	Livestock deaths	7.81	0.88	0.50	1.00	0.
	Milk production	22.00	0.84	0.83	0.71	0.77
	Food insecurity	11.11	0.89	1.00	1.00	1.00
	Crop losses	9.21	0.89	1.00	0.33	0.50
	Trekking distance water	26.79	0.77	0.50	0.50	0.50
	Malnutrition	32.00	0.70	0.60	0.75	0.67
Semi-arid	Pasture	12.93	0.90	0.82	0.95	0.88
	Livestock deaths	12.07	0.86	0.69	0.65	0.67
	Milk production	22.22	0.74	0.33	0.17	0.22
	Food insecurity	13.83	0.86	0.25	0.11	0.15
	Crop losses	9.02	0.90	0.20	0.25	0.22
	Trekking distance water	37.50	0.67	0.50	0.60	0.55
	Malnutrition	32.43	0.66	0.60	0.55	0.57
Sub-humid	Pasture	6.25	0.92	0.93	1.00	0.96
	Livestock deaths	1.19	0.98	0.50	0.67	0.57
	Milk production	19.64	0.82	0.90	0.82	0.86
	Food insecurity	18.33	0.80	0.17	0.33	0.22
	Crop losses	5.00	0.94	0.00	0.00	NA
	Trekking distance water	12.12	0.83	1.00	0.60	0.75
	Malnutrition	29.63	0.72	0.37	0.43	0.40

~~The occurrence of drought impacts in Trekking distance for water can be best predicted for the counties Narok and Nyeri with an AUC of 0.88. The models of the semi-arid counties of Baringo, Kitui and Kwale performed relatively poorly with the exception of the model developed for Crop losses (0.84).~~

Figures 4 ~~and~~, 5 ~~show the~~ and 6 show the top five drought indices which are best linked with the drought impact categories ~~; we take into account only the relations of the best performing models. The MeanDecreaseAccuracy (MDA: in %) represents the importance of the predictor for the model: it expresses how much accuracy the model loses when each variable would be excluded one by one. The mean decrease in Gini coefficient is a measure of how each variable contributes to the homogeneity of the nodes and leaves in the Random Forest. In this regard, homogeneity means that most of the samples at each node are from one class. A higher MeanDecreaseGini (in %) indicates higher explanatory importance.~~
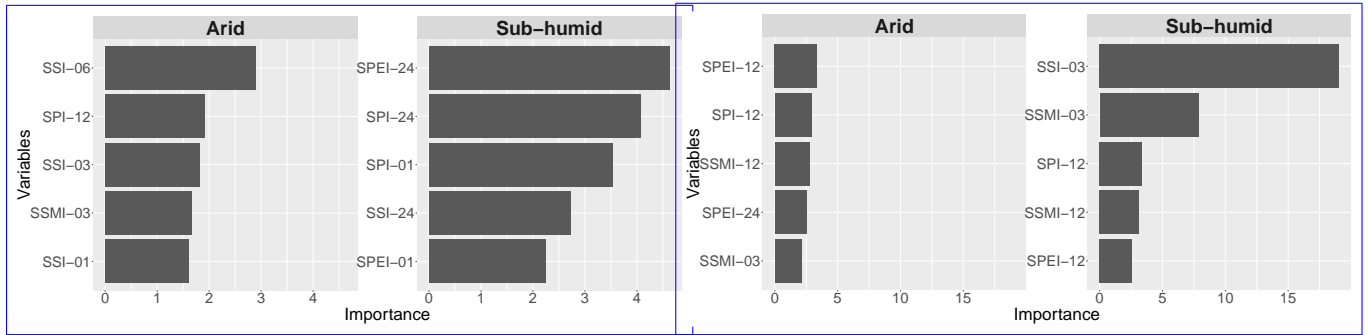
(a) Pasture

(b) Livestock deaths

Figure 4. Drought indices best linked with Pasture and Livestock deaths for ~~the arid region (~~Marsabit~~)~~ and ~~the sub-humid regions~~ (Narok/Nyeri~~. MeanDecreaseAccuracy (in %)indicates how much accuracy the model would loose when each variable would be excluded.The MeanDecreaseGini (in %) presents how each variable contributes to the homogeneity of the nodes and leaves in the Random Forest.~~
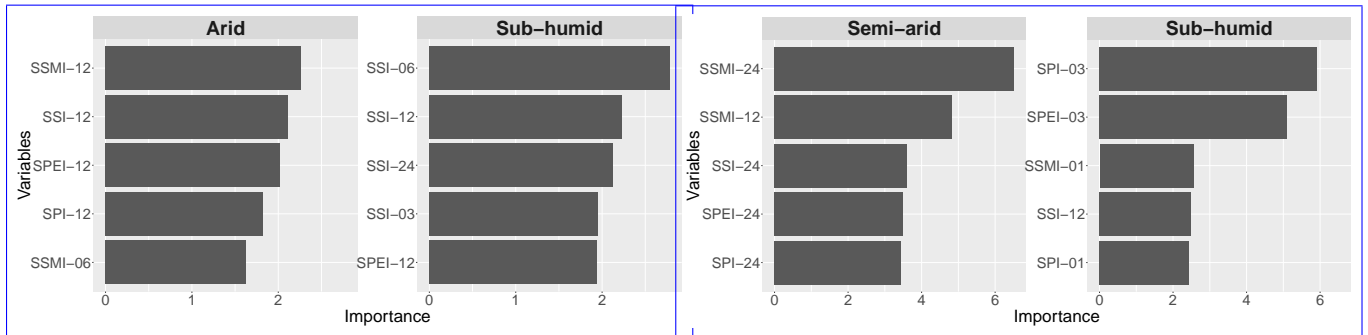
(a) ~~Food insecurity (MA)~~Milk production

(b) Crop losses~~(BA, KW, KI)~~

Figure 5. ~~Trekking distance water points~~ Drought indices best linked with Milk production for the arid region (~~NA~~Marsabit) and sub-humid regions (Narok/~~NY~~Nyeri) and drought indices best linked with Crop losses for the semi-arid regions (Baringo, Kitui and Kwale) and sub-humid regions.

~~Drought indices best linked with Trekking distance water points (NA/NY), Crop losses (BA, KW, KI) and Food insecurity (MA).~~

~~.~~ As shown in Figure 4a, Pasture impacts for ~~Marsabit~~ the arid region tend to be related to shorter drought anomalies (6 months) than ~~Narok and Nyeri~~ the sub-humid regions (24 months). Furthermore, SSI ~~is the best predictor~~ and SPI are the best predictors for Pasture impacts in ~~Marasbit while the meteorological drought indices SPI and SPEI~~ the arid region while SPEI and SPI are the best predictors for ~~Narok and Nyeri. SPEI-24 is by far the best performing drought indicator for Pasture in Narok/Nyeri with a MDA higher than 18%~~the sub-humid regions. For Livestock Deaths (Figure 4b), the situation is reversed: ~~meteorological indices such as SPEI and SPI with~~ longer accumulation periods (12–24 months) are ~~the best link for Marsabit while the predictors SSI and SSMI with~~ designated to the arid region while shorter accumulation periods are related to the
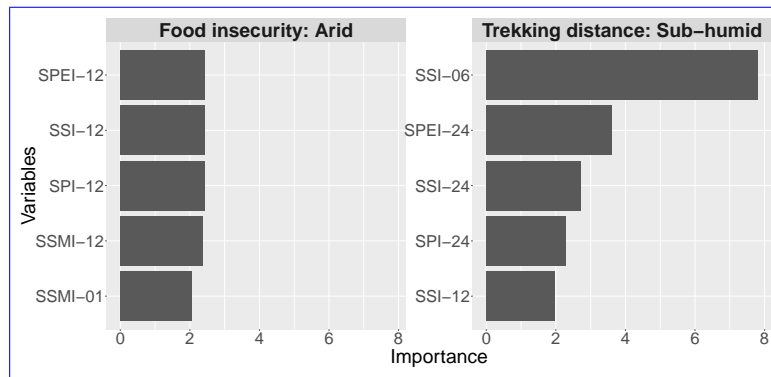
Figure 6. Drought indices best linked with Food insecurity for the arid region (Marsabit) and the drought indices best linked with Trekking distance for water for the sub-humid regions (Narok/Nyeri).

sub-humid regions (3–12 months). SPEI and SPI are the best ~~link for Narok and Nyeri. SPEI-12 is by far the best performing~~
~~drought indicator in Marsabit for Livestock deaths.~~
    ~~The results show that Food insecurity for~~ predictors for Livestock deaths in the arid region while SSI and SSMI are the best predictors for the sub-humid regions. Especially SSI-03 seems to be a strong predictor (importance of 19.05) for Livestock deaths in the sub-humid region. Milk production in the arid region ~~of Marsabit can be well predicted with~~ tend to be most related to accumulation periods of 12 months in relation to a range of drought indices ~~(Figure 5a), among which SSMIis the~~
~~main drought predictor. However, the accumulation period is more or less stable on 12~~ , namely SSMI, SSI, SPEI and SPI. At the sub-humid regions, SSI is the best predictor for Milk production with accumulation periods between 3–24 months. For ~~Baringo, Kwale and Kitui,~~ the semi-arid regions, high accumulation periods (~~6–24~~ 12–24 months) are associated with Crop losses ~~, whereby SSMI , SSI~~ whereby SSMI is the most prominent predictor. For the sub-humid regions, lower accumulation periods (01-12) are associated with Crop losses whereby SPI and SPEI are the most prominent ~~indices (Figure 5b). Noticeable~~
~~is that SSMI-24 is by far the most prominent drought indicator for Crop Losses with a MeanDecreaseAccuracy of 24% and a~~
~~MeanDecreaseGini of 10%~~predictors. The results show that Food insecurity for the arid region can be well predicted with a range of drought indices (Figure 5a), namely SPEI, SSI, SPI and SSMI with a more or less stable accumulation period of 12 months. Trekking distance to water points for ~~Narok/Nyeri~~ the sub-humid regions can mainly be predicted by SSI ~~, SPEI and~~
~~SPI~~ with an accumulation period ~~between 6–24 months(Figure 5c)~~of 6 months.

4 Discussion

4.1 Data sources and methods

This study used the water scarcity dataset of McNally et al. (2019) which is based on regional streamflow data and population data from WordPop 2015. This dataset has never been validated in the Horn of Africa which could be a limitation of this

research. In addition, different hydrological datasets were used for the water scarcity dataset and the calculation of the SSI.
However, despite some inconsistencies between the datasets, both are following the same pattern which justifies drawing conclusions based on the water scarcity dataset. The comparison between streamflow data of the water scarcity dataset and SSI-01 is included in Appendix B. Furthermore, the computation of the meteorological drought indices (SPI/SPEI) and the WS dataset are based on different satellite-based precipitation products, namely MSWEP and CHIRPS respectively. The two datasets showed good performances on global level (Beck et al., 2017b) and more specifically for East Africa (Cattani et al., 2021). Although the slightly underestimation of the MSWEP data compared to CHIRPS over East Africa, both precipitation products showed considerable agreement (Cattani et al., 2021), thereby justifying the simultaneous use of both products.

Drought impact data have been generated by analyzing the monthly county-specific reports of the NDMA. ~~These reports had some monthly gaps and were sometimes written in different formats which made it hard to objectively appraise the drought impacts and their magnitude. However, iterative processes and focusing on abnormal conditions caused by drought according to the NDMA ensures~~ This data source had some missing months, namely between 4 and 8 months, different per county, and mainly at the beginning of the period (between July 2013 and December 2014). Despite these missing months, there is still a robust and reliable timeline of drought impact data available for more than 90% of the considered months. In addition, the bulletins were iteratively checked by several NDMA employees to ensure a reliable list of drought impact ~~occurrences~~data. Despite the great effort and very valuable drought impact data information from the NDMA, this study stresses the need for an impact database for Africa such as the already existing databases EDII ~~and DIR~~ (EDC, 2013) and DIR (NDMC, 2005) for Europa and the USA respectively. Future research can assess how to build an impact database with enhanced quality in terms of higher spatial and temporal resolution, more impact categories and more quantitative information on the impact. To build such a database for historical events, systematically blending and fusing impact data coming from different sources need to be explored (Majani et al., 2022). Sources that can possibly complement the NDMA bulletins range from global repositories such as the Emergency Events Database (EM-DAT~~or DesInventar,~~) (Guha-Sapir et al., 2016) or the Disaster Inventory System (DesInventar, https://www.desinventar.net/), drought appeals from humanitarian organisations such as the Kenya Red Cross Society, index-insurance claims submitted to insurance companies or digital media reports.

We used a Random Forest technique to link drought impacts with drought indices. However, other literature used other techniques such as the Pearson correlation (Wang et al., 2020), Spearman correlation (Ma et al., 2020), and logistic regression (Bachmair et al., 2017; Blauhut et al., 2015; Stagge et al., 2015). Using RF to link drought indices with drought impacts is a fairly new technique ~~and has only been done before by Bachmair et al. (2016, 2017) with a focus on Germany and the UK~~but has been done several times before (e.g. Bachmair et al. 2016, 2017; Wang et al. 2020). These studies indicated a potential of using RF for drought M&EW. This study confirms this, as the performance ~~indices (AUC)~~metrics were good for several drought impact categories and all the discussed models in terms of 'variable importance' showed similarities with the results of the point-biserial correlation (Appendix C). However, ~~using RF to link drought impacts with drought indices also shows the need to expand the drought impact~~ there were differences in the predictive power of the RF model among the drought impact categories and the regions. This could be related to (1) data availability (e.g., data on impacts related to malnutrition) as the RF model is sensitive to data ~~collection because of its sensitivity to data~~availability (Bachmair et al., 2016) and (2) deviations

in the link between drought impacts and indices among the counties, making the model perform worse when the counties are combined together (i.e., the models in relation to the semi-arid regions).

4.2 Relations with aridity

The majority of the drought impact data are livestock- and pasture-related . It was expected that the reported drought impacts were linked which is in accordance with the main livelihood activity of the county. This is partly confirmed by the results of this study. The main livelihood activity of Marsabit is pasture whereby around 50% of the drought impacts are related to this activity. Nyeri (Kieni sub-county) has agro-pastoral activities and more than 60% of the reported drought impacts is related to pastoral activities. Most of the reported drought impacts are related to pastoral activities, this could be due to the drought impact categories considered considered counties and with the information provided by the NDMA.

Marsabit and Kitui had the highest reported drought impacts while Baringo and Nyeri the least amount of reported drought impacts. This suggests that drought impacts are linked with aridity because Marsabit and Kitui contain larger areas classified as (semi-)arid than Baringo and Nyeri. The Also, the interference with socio-economic circumstances is likely to play a role as acute and chronic food insecurity, poverty, lack of economic development, limited access to basic social services, and low education levels are the highest among households in the ASALs (FEWS NET, 2013).

Drought impacts often appeared after the onset of a drought, therefore introducing a kind of lag. Maliva and Missimer (2012) stated that arid areas will have more extreme drought due to global warming which will increase the potential evapotranspiration (Seneviratne et al., 2021; Wang et al., 2022). However, this study can not link drought occurrence to aridity cannot link the frequency and intensity of drought events with different aridity levels because of the short timeframe (10 approx. 7 years) analyzed. The analysis of longer timeseries could time series could not only indicate if there is an interannual trend and variability of drought indices, therefore determining whether are changes in drought severity, area, and frequency but also if there is a drying climate or a drought event long-term shift to a more arid climate (Xu et al., 2021). This could be an interesting follow-up research whereby aridity conditions could be analysed in relation to drought occurrences.

4.3 Water scarcity and drought impacts

According to the water scarcity dataset, most drought impacts occurred at times without water stress (Figure 3b.), with the exception of Nyeri. These findings contrast with the text-based drought impact data on distance from water sources (i.e., Trekking distance for water) from the NDMA bulletins, which could be used as a proxy for water stress conditions. Increased distance from water sources was reported in arid and semi-arid regions the arid (Marsabit) and sub-humid (Nyeri) region during most of the months when meteorological and hydrological drought conditions occurred (Figure 3b). The same impact was reported for three months during the 2017–2018 drought period and one month during the 2019 drought event in Nyeri (Figure 2b2). Noticeable is that Marsabit has more reported drought impacts on Trekking distance for water (16.9%) than Nyeri (9.1%) (Table 2) while Nyeri has more months with water scarcity than Marsabit which has zero months with water scarcity (Figure 3a.).

The discrepancies between the increased distance from water sources and the water scarcity index could be explained by the fact that the streamflow data used for developing the WS dataset were calculated without taking into account the presence of reservoirs, located mainly in the central-western areas of Kenya (Lehner et al., 2011; Mulwa et al., 2021). In addition, the WS dataset uses population data as a proxy for water demand. Since the population density has high values in central-western

500 counties and low values for the ASAL counties (which host only 25% of the population although they cover about 80% of the territory of Kenya ; (FEWS NET, 2013))(FEWS NET, 2013), it is not surprising that the WS index is higher for west-central counties than for ASAL counties. However, low population density does not imply low water stress: pastoral and agricultural livelihoods are predominant in the ASAL counties and are highly dependent on water availability (FEWS NET, 2013). In addition, the staple foods 'pulses' (i.e. dry cereals) for densely populated areas located in central-western counties are mainly

505 supplied by the ASAL counties, resulting in high water consumption by the latter. Finally, water scarcity is also shaped by political choices, public policies, and social order (Savelli et al., 2021; Van Loon and Van Lanen, 2013). These factors were not accounted for in the development of the WS dataset.

In summary, the WS dataset is apolitical, does not take reservoirs into account, and is highly dependent on population density, which is not a true reflection of water demand. Despite these limitations, interesting conclusions can still be drawn.

510 The WS dataset highlights suggests that water resources were sufficient to meet the water demand in the arid and semi-arid regions of Kenya during drought events. However, water insecurity in the ASAL regions was high during periods of drought (FEWS NET, 2017), possibly due to inefficient water management, for example poor maintenance of water supply systems (related in turn to corruption and poverty) (Bellaubi and Boehm, 2018; Jenkins, 2017; Mulwa et al., 2021). The sub-humid central-western counties, on the other hand, should have suffered from could have experienced water scarcity during periods

515 of drought due to the high population density and hence the high pressure on available water resources. However, in reality, they experience little water stress thanks to the presence of reservoirs that buffered the drought conditions (FEWS NET, 2017). This shows that water scarcity can be reversed through wise usage of the available water resources (Phillip, 2013).

4.4 Drought indices and the Random Forest model

The results show that linking drought indices with drought impacts is region-specific, as confirmed by many other studies

520 (Bachmair et al., 2015, 2016, 2018; Blauhut et al., 2015; Ma et al., 2020; Parsons et al., 2019; Stagge et al., 2015; Wang et al., 2020). For instance, shorter accumulation periods were found for Pasture at Marsabit (SSI-06) while longer accumulation periods were found for Narok/Nyeri (SPEI-24). This lag suggests the presence of water buffers in Narok/Nyeri, damming the sub-annual fluctuations in water availability and therefore generating less influence on the impact category Pasture (Mulwa et al., 2021). On the contrary, Livestock deaths are linked with high accumulation periods in Marsabit (SPEI-12) and short

525 accumulation periods in Nyeri (SSI-03). These differences between the in best match between drought impacts and drought indices implies therefore imply a link with human activities as they can lag the moment of impact occurrence. As confirmed by Xu et al. (2019), human activities can interfere with natural processes and therefore influence the drought propagation time between meteorological and hydrological drought. This calls for more research towards water management practices in relation to drought indices and drought impacts.

530 Regarding the drought indices, various drought indices are marked as the most optimal indicator: SSI is found in relation to Pasture (arid region), Livestock deaths (~~Marsabit), Pasture (Narok/Nyeri~~ sub-humid regions), Milk production (sub-humid regions) and Trekking distance to water points (~~Narok/Nyeri~~ sub-humid regions), while SSMI is found in relation to Milk production (arid region) and Crop losses (~~Baringo, Kwale, Kitui) and Food insecurity (Marsabit~~ semi-arid regions). Noticeable is that SSI gives a possible link with water-dependent activities while SSMI shows a possible link with agricultural practices.

535 It is expected that SSI and SSMI would show a memory in relation to SPI and SPEI because of the propagation through the hydrological cycle, introducing a lag between meteorological, soil moisture and hydrological drought ~~(Wang et al., 2016)~~ (Seneviratne et al., 2012; Wanders et al., 2017; Wang et al., 2016). Therefore, the time length and duration of SPI and SPEI can be used to express soil moisture and hydrological drought. In general a 1-month timescale is considered meteorological drought, 3-6 months as soil moisture drought and 12 months can be considered as hydrological drought (Dai et al., 2020). This

540 link is partly visible by looking at the drought indices in relation to the accumulation periods. For instance, SSI-06 is the best match for Trekking distance household which indicates hydrological drought. The best link after SSI-06 are amongst others SPEI and SPI with a 24 months timescale, also indicating the presence of a hydrological drought.

  Studies that linked drought impacts with drought indices are mainly focused on Europe (Bachmair et al., 2015, 2016, 2018; Blauhut et al., 2015; Parsons et al., 2019; Stagge et al., 2015) and recently China (Ma et al., 2020; Wang et al., 2020). Com-

545 parisons with these studies are quite difficult due to the different socio-economic and climatic circumstances. As studied by Bachmair et al. (2018), SPI and SPEI with an accumulation period of three and four months showed the highest correlation for the impacts on crops in Germany. This is ~~not~~ consistent with the results found in ~~this study in~~ relation to Crop losses for ~~Baringo, Kitui and Kwale: those~~ the sub-humid regions whereby SPI-03 and SPEI-03 are the best match. However, it is not consistent with the results found for the semi-arid regions whereby the accumulation periods are quite high (~~6–24~~ 24 months).

550 As stated in the study of Bachmair et al. (2018), an accumulation period of one month was found to have a notably lower correlation with drought impacts and was often non-significant which is also confirmed by the results of this study. A reasonable explanation for this is that the occurrence of impacts lags behind the occurrence of drought. Another study of Bachmair et al. (2016), showed that SPI and SPEI with longer accumulation periods (12–24 months) are best linked to impact occurrence in the UK when using the RF model. In general, this does match with the results of this study ~~:~~ whereby SPI-12, SPEI-12,

555 SPI-24 and SPEI-24 are ~~the most occurring accumulation periods,~~ often present in the top five drought indices best linked with the drought impact categories, thereby linking the occurrence of drought impacts with the presence of hydrological drought. Our results indicate that impacts associated with different types of drought have different response times, as confirmed by the distinct differences in drought indices and impact linkage pattern.

  ~~It should be noted that~~ This study did not directly account for short and/or long term drought resilience actions applied in the

560 ASAL regions and their link to the reported drought impacts in the NDMA monthly bulletins while this could be of influence on the drought impacts-indices relationship. Drought resilience actions can be related to (1) structural interventions for increasing the water availability (e.g. construction of reservoirs), (2) sustainable land management practices (e.g. inter-cropping, agroforestry and drought resistant crops), (3) pasture and livestock management (e.g. livestock restocking and improved varieties of grass) and (4) livelihood diversification (Kenya, 2016; Mude et al., 2007; Njarui et al., 2020; Opiyo et al., 2015; Parry, 2016; weADAPT, 2023)

565 . Such adaptation measures can ~~influence the optimal drought index found by using the RF model. The use of adaptation measures is linked with increasing livelihood resilience whereby smallholders are better prepared for future challenges (Nyberg et al., 2020)~~ increase the resilience of the communities (Nyberg et al., 2020). This could as well explain the differences in the optimal drought indices found among the researched areas as the level of preparedness can lag or mitigate the occurrence of drought impacts, resulting in a better fit with drought indices with higher accumulation periods. The past years Kenya has experienced

570 several drought events. This can influence the extent of adaptation measures taken and therefore the resilience against droughts which affects the impacts. It is therefore recommended to link adaptation measures to drought impacts and indices in order to analyze spatial differences and to map fluctuations over time.

This study contributes to the ongoing debate about the operational needs for drought monitoring by linking multiple drought indices to reported drought impacts. ~~Results~~ Our results show the best drought index for a given impact~~which~~. This can be

575 combined with other socio-economic and environmental data to provide enough inputs for the construction of drought impact forecasting, useful for stakeholders and decision makers (Heinrich and Bailey, 2020; Stagge et al., 2015). In addition, this research takes ~~first steps in analysing~~ the first step in exploring the link between drought and water scarcity and aridity, which is valuable information for the existing literature database on drought and its impacts. However, it is recommended to validate the results in other areas and on finer spatial scales whereby the influence of human activities on drought propagation and water

580 scarcity can be analyzed. Besides this, research would benefit from a refinement of the water scarcity dataset in order to better represent human influences on water scarcity conditions.

5   Conclusions

~~Drought is expected to happen more frequently in the future, generating a range of impacts in diverse sectors. This urges the~~ There is an urgent need to develop early warning systems to mitigate the adverse consequences of drought and thereby reducing

585 the human and financial costs. However, there is still no full understanding of the relation between drought impacts and drought indices in Africa. ~~In addition, this~~ This continent struggles with water scarcity and the presence of arid regions, which possibly influences the relation between drought hazard and impacts. This paper aimed to fill this knowledge gap by exploring the link between drought impacts, drought indices, water scarcity and aridity with a focus on Kenya.

The arid region of Marsabit had the most severe drought and the highest amount of drought impacts over a timeframe from

590 2016 to 2020. Nyeri, classified as a sub-humid region, had lower frequencies and intensities of drought and reported the least amount of drought impacts. This indicates that drought impacts are linked with drought severity and that the occurrence of drought impacts are related to aridity. The skewed spatial distribution of drought impacts could be related to the fragile socio-economic conditions in the ASALs of Kenya which makes this region more vulnerable to drought than the sub-humid region of central-western Kenya. Water scarcity as derived by the WS dataset was not found to be related with aridity while this

595 was expected ~~due to the presence of unreliable water conditions~~because arid regions are often facing limited water resources. On the contrary, Marsabit (arid) did not experience any water scarcity during the analysed timeframe (March 2018 and 2020) whilst Nyeri (sub-humid) did. In addition, most drought impacts occurred at times without water stress (except for Nyeri)

even when increased distance from water sources was reported as a drought impact, which can be used as a proxy for water stress conditions. Reasonable explanations for this can be found in the water scarcity dataset which is apolicital, does not take reservoir into account, and is highly dependent on population density.

With a Random Forest model, a link between drought impacts and drought indices was made. The results indicated that every region, aggregated on aridity, had their own set of predictors for every impact category. Region dependency was found by other studies as well. In relation to drought impacts on Pasture, anomalies were shorter (6 months) for the arid region of Marsabit than for the sub-humid regions of Narok/Nyeri (24 months). For the impacts on Livestock deaths reversed results were found: lower accumulation periods were found for Narok/Nyeri (3-12 months) while longer accumulation periods were present in Marsabit (12-24 months). Drought indices with longer timescales ($>\geq$ 12 months), indicating a hydrological drought, were often found to match best with ~~all~~ the drought impact occurrences. The differences in linkages could be related to water management practices, natural characteristics and climatic circumstances.

The predictive ability of indices heavily depends on the spatial and temporal resolution of drought impact data. Therefore, this study stresses the need of systematic drought impact data collection ~~as done by the NDMA~~around the world following the example of the NDMA in Kenya. In addition, ~~a finer spatial resolution is needed~~ we recommend to look at finer spatial resolutions to capture the regional differences in human influences on water scarcity and drought impacts. Studying ~~other~~ similar research areas and validating the results of this study on smaller scales will expand the knowledge base on drought and impacts and will substantiate the conclusions of this study. This study analyzed the link between drought indices and text-based impact reports with a focus on the African continent which has never been studied before. The integration of regional predictions on drought impacts will contribute to the development of early warning systems on drought which help society to better prepare and act accordingly, therefore reducing vulnerability and increasing resilience to drought and impacts.

Appendix A: Detailed explanation of the water scarcity dataset

The water scarcity index from McNally et al. (2019) is based on outputs from the FEWS NET Land Data Assimilation System (FLDAS), which is a custom instance of the National Aeronautics and Space Administration (NASA) Land Information System (LIS). The FLDAS's Noah 3.6 land surface model is driven by the Climate Hazards Group InfraRed Precipitation with Station (CHIRPS) rainfall and NASA's Modern-Era Retrospective analysis for Research and Applications (MERRA-2) meteorological forcing. This model partitions rainfall inputs into surface and subsurface runoff (i.e., baseflow), soil moisture storage and evapotranspiration. Surface runoff is the precipitation in excess of infiltration and saturation capacity of the soil while subsurface runoff is the drainage from the bottom soil moisture layer caused by gravity. The total runoff is routed though the river network with the Hydrological Modelling and Analysis Platform version 2 (HyMAP-2) river routing scheme. The definition of catchments are based on boundaries defined by the U.S. Geological Survey (USGS) Hydrological Derivatives for Modelling Applications (HDMA) database. A Pfafstetter code, based on an hierarchical numbering system, are attributed to the catchments. For the water scarcity index, Pfafstetter level 6 basins are used in order to represent the relatively local nature of water supplies. Two population datasets are used as a proxy for water demand, namely the WorldPop 2015 dataset and the European Commission's Joint Research Center's (JRC) Global Human Settlement (GHS) data. To classify the amount of water scarcity, the Falkenmark index is used. The Falkenmark Index thresholds are specified annually while monthly data is required for the routinely updated maps about water scarcity. Therefore, a 12-month running total of the streamflow from the current and 11 previous months are used whereby the Falkenmark index (based on yearly values) can still be used on a monthly resolution. The population estimates are aggregated to Pfafstetter basin level 6 whereafter the 12-month total spatially aggregated streamflow (m^3) is divided by the population to produce an estimate of m^3/person (McNally et al., 2019).

(a) Marsabit   (b) Nyeri
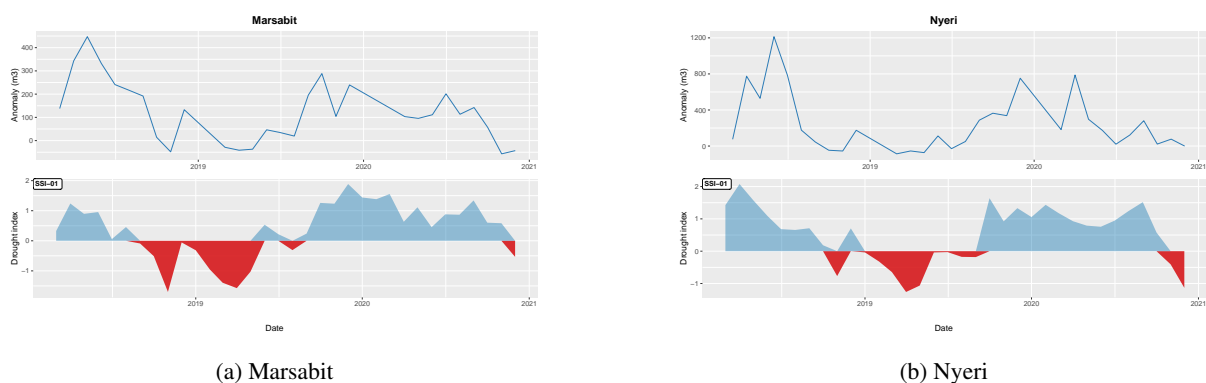
Figure A1. Streamflow anomalies (WS) and SSI-01 between March 2018 and 2020.

Appendix B: The hydrological datasets: the streamflow datasources

Different hydrological datasets were used for the water scarcity dataset and the calculation of the SSI. The SSI index is based on data from GloFAS while streamflow data for the water scarcity dataset is based on outputs from the FLDAS. If there are any discrepancies between the datasets, wrong conclusions could be made. To compare the two different datasets, SSI-01 is plot together with the streamflow anomalies of the water scarcity dataset for Marsabit and Nyeri (Figure A1). The streamflow
645 anomalies are based on the 1982-2016 FLDAS historical record while SSI is based on the period between 1980 and 2010. Despite some irregularities between the datasets, both are following quite the same pattern. This suggest that it is reasonable to compare the results from the two different hydrological datasets.

Appendix C: ~~A detailed explanation about the Random Forest model~~Point-biserial correlation

~~Random forest (RF) is a machine learning algorithm whereby a large number of regression or classification trees on bootstrapped~~
650 ~~sub-samples of the data are constructed. Bootstrapping is a way to resample the dataset which includes replacement from the original dataset. In other words, RF's combines several randomized decision trees and aggregates their predictions by averaging. The goal of a decision tree is to create a model that predicts the value of a target by learning simple decision rules induced from the data features. A decision tree consists of nodes, edges/branches and leaf nodes. The nodes are the test for the value of a certain attribute (predictor), the edges/branches are the outcome of a test and connect to the next node or leaf and the leaf~~
655 ~~nodes are the terminal nodes predicting the outcome. In~~ In order to validate the ~~model, a training data set and a test dataset is constructed with a proportion of 75% and 25% of the original dataset. Each tree is built on a subset of the training data set: approximately two-third of the training dataset is used for building a tree while one third is not used, called the out-of-bag error data. This generates an additional estimate of performance, namely the out-of-bag error which is a method~~ results of the RF model in relation to variable importance, a point-biserial correlation was conducted. It is used to measure the ~~prediction error~~
660 ~~of the random forest. For the model, two parameters needed to be tuned, namely the amount of randomized trees (ntree) and the amount of variables available for splitting at each tree node (mtry). The value of ntree has been proven to have not much effect on the overall accuracy of the model and is set to the default value of ntree = 500. For the best value of mtry, the function tuneRF function of the RandomForest package has been used which aims to lower the OOB error. The tuned parameters for mtry are visible in~~ relationship between a binary and continuous variable. Table A1. shows the results of the point-biserial
665 correlation: only the top 5 drought indices with the strongest correlation are included. The minus sign indicates a negative correlation between the two variables.
~~The performance of the various models for the impact categories were tested by applying the model on the test set data (25% of the original data set). The AUC (Area Under the Curve) ROC (Receiver Operating Characteristics) curve was used to check and visualize the performance. It describes how much the model is capable of distinguishing between the classes: how higher~~
670 ~~the AUC, the better the model is at predicting 0 classes as 0 and 1 classes as 1. The ROC curve is plotted with the Sensitivity on the y-axis and Specificity on the x-axis. These variables represent the true positives and true negatives respectively.~~

Data availability. Data is available on the 4tu.ResearchData platform. The DOI and link of access is https://doi.org/10.4121/19620357.

Author contributions. MRL has designed and conducted the research, supervised by RT, AvL, AS and AT. RO calculated, provided and have written the data on the drought indices. MRL has written the manuscript with input from all co-authors. MvdH, CW and SW have reviewed the manuscript. The final version has been approved by all co-authors.

Competing interests. The contact author has declared that neither they nor their co-authors have any competing interests.

Acknowledgements. We would like to thank Amy McNally for providing the water scarcity dataset. In addition, thanks to the National Drought Management Authority (NDMA) of the Kenyan government for providing the data for the drought impacts.

Table A1. Point-biserial correlation: linking the drought indices with drought impact category per region with the same level of aridity. The asterisks indicate the statistical significance: $p < 0.05$*, $p < 0.001$* and $p < 0.0001$***.

		Pasture		Livestock deaths		Milk production		Food insecurity		Crop losses		Water distance		Malnutrition	
Arid	SSI-06	-0.53***	SPEI-12	-0.48***	SSI-12	-0.56***	SSI-12	-0.67***	SPI-06	-0.12	SSI-03	-0.30*	SSMI-12	-0.09
	SSMI-01	-0.53***	SPI-12	-0.46***	SSI-06	-0.53***	SPEI-12	-0.64***	SPEI-06	-0.09	SPEI-06	-0.27*	SPEI-12	-0.04
	SPEI-12	-0.51***	SSMI-12	-0.39**	SPEI-12	-0.53***	SPI-12	-0.63***	SPI-01	-0.05	SSI-06	-0.26*	SPI-12	-0.02
	SSI-01	-0.50***	SSMI-06	-0.38**	SPI-12	-0.52***	SSI-06	-0.61***	SPEI-01	-0.05	SPI-06	-0.24	SSMI-24	-0.02
	SSI-12	-0.50***	SSI-12	-0.32*	SSMI-06	-0.49***	SSMI-03	-0.61***	SSI-06	-0.04	SSI-01	-0.24	SSMI-06	-0.01
Semi-arid	SSMI-24	-0.25*	SSMI-03	-0.20	SPI-03	-0.20	SSMI-06	-0.18	SSI-24	-0.17	SPI-06	-0.22*	SPEI-03	-0.18
	SPI-24	-0.23*	SPI-06	-0.20	SPEI-03	-0.18	SSMI-03	-0.16	SSMI-24	-0.17	SPEI-06	-0.21*	SPI-03	-0.16
	SPEI-24	-0.18	SSMI-01	-0.19	SSMI-06	-0.17	SSMI-12	-0.14	SSI-12	-0.15	SPI-12	-0.20	SPEI-01	-0.12
	SSMI-12	-0.14	SSMI-06	-0.18	SPI-12	-0.16	SPI-12	-0.11	SPEI-24	-0.13	SPI-01	-0.19	SSI-03	-0.11
	SSMI-06	-0.11	SPEI-06	-0.18	SPEI-12	-0.16	SPEI-12	-0.11	SSMI-12	-0.10	SPEI-12	-0.18	SSI-01	-0.11
Sub-humid	SPEI-24	-0.46***	SSI-03	-0.56***	SSI-06	-0.58***	SPEI-24	-0.19	SPEI-03	-0.30*	SSI-06	-0.48***	SPEI-03	-0.22
	SPI-24	-0.42***	SPEI-06	-0.50***	SPEI-12	-0.50***	SPI-24	-0.17	SPI-03	-0.29*	SPI-24	-0.42***	SPI-03	-0.22
	SSMI-24	-0.20	SPI-06	-0.48***	SPI-12	-0.50***	SSI-24	-0.13	SPEI-01	-0.20	SPEI-24	-0.38**	SSMI-01	-0.21
	SSI-24	-0.19	SSMI-01	-0.45***	SSI-12	-0.47***	SSI-06	-0.12	SPI-01	-0.19	SSI-12	-0.36**	SPI-06	-0.21
	SSMI-03	-0.16	SSI-06	-0.44***	SSI-03	-0.46***	SSI-01	-0.10	SSMI-01	-0.18	SSI-24	-0.36**	SPEI-06	-0.20

References

Atzberger, C. and Eilers, P. H.: Evaluating the effectiveness of smoothing algorithms in the absence of ground reference measurements, International Journal of Remote Sensing, 32, 3689–3709, https://doi.org/10.1080/01431161003762405, 2011.

Atzberger, C., Formaggio, A., Shimabukuro, Y., Udelhoven, T., Mattiuzzi, M., Sanchez, G., and Arai, E.: Obtaining crop-specific time profiles of NDVI: the use of unmixing approaches for serving the continuity between SPOT-VGT and PROBA-V time series, International Journal of Remote Sensing, 35, 2615–2638, https://doi.org/10.1080/01431161.2014.883106, 2014.

Ayugi, B., Tan, G., Niu, R., Dong, Z., Ojara, M., Mumo, L., Babaousmail, H., and Ongoma, V.: Evaluation of meteorological drought and flood scenarios over Kenya, East Africa, Atmosphere, 11, 307, https://doi.org/10.3390/atmos11030307, 2020.

Bachmair, S., Kohn, I., and Stahl, K.: Exploring the link between drought indicators and impacts, Natural Hazards and Earth System Sciences, 15, 1381–1397, https://doi.org/10.5194/nhess-15-1381-2015, 2015.

Bachmair, S., Svensson, C., Hannaford, J., Barker, L., and Stahl, K.: A quantitative analysis to objectively appraise drought indicators and model drought impacts, Hydrology and Earth System Sciences, 20, 2589–2609, https://doi.org/10.5194/hess-20-2589-2016, 2016.

Bachmair, S., Svensson, C., Prosdocimi, I., Hannaford, J., and Stahl, K.: Developing drought impact functions for drought risk management, Natural Hazards and Earth System Sciences, 17, 1947–1960, https://doi.org/10.5194/nhess-17-1947-2017, 2017.

Bachmair, S., Tanguy, M., Hannaford, J., and Stahl, K.: How well do meteorological indicators represent agricultural and forest drought across Europe?, Environmental Research Letters, 13, 034 042, https://doi.org/10.1088/1748-9326/aaafda, 2018.

Baig, M. R. I., Naikoo, M. W., Ansari, A. H., Ahmad, S., Rahman, A., et al.: Spatio-temporal analysis of precipitation pattern and trend using standardized precipitation index and Mann–Kendall test in coastal Andhra Pradesh, Modeling Earth Systems and Environment, 8, 2733–2752, https://doi.org/10.1007/s40808-021-01262-w, 2022.

Balsamo, G., Beljaars, A., Scipal, K., Viterbo, P., van den Hurk, B., Hirschi, M., and Betts, A. K.: A revised hydrology for the ECMWF model: Verification from field site to terrestrial water storage and impact in the Integrated Forecast System, Journal of hydrometeorology, 10, 623–643, https://doi.org/10.1175/2008JHM1068.1, 2009.

Barrett, A. B., Duivenvoorden, S., Salakpi, E. E., Muthoka, J. M., Mwangi, J., Oliver, S., and Rowhani, P.: Forecasting vegetation condition for drought early warning systems in pastoral communities in Kenya, Remote Sensing of Environment, 248, 111 886, https://doi.org/10.1016/j.rse.2020.111886, 2020.

Beck, H. E., Van Dijk, A. I., Levizzani, V., Schellekens, J., Miralles, D. G., Martens, B., and De Roo, A.: MSWEP: 3-hourly 0.25 global gridded precipitation (1979–2015) by merging gauge, satellite, and reanalysis data, Hydrology and Earth System Sciences, 21, 589–615, https://doi.org/10.5194/hess-21-589-2017, 2017a.

Beck, H. E., Vergopolan, N., Pan, M., Levizzani, V., Van Dijk, A. I., Weedon, G. P., Brocca, L., Pappenberger, F., Huffman, G. J., and Wood, E. F.: Global-scale evaluation of 22 precipitation datasets using gauge observations and hydrological modeling, Hydrology and Earth System Sciences, 21, 6201–6217, https://doi.org/10.5194/hess-21-6201-2017, 2017b.

Beck, H. E., Wood, E. F., Pan, M., Fisher, C. K., Miralles, D. G., Van Dijk, A. I., McVicar, T. R., and Adler, R. F.: MSWEP V2 global 3-hourly 0.1 precipitation: methodology and quantitative assessment, Bulletin of the American Meteorological Society, 100, 473–500, https://doi.org/10.1175/BAMS-D-17-0138.1, 2019.

Beguería, S., Vicente-Serrano, S. M., Reig, F., and Latorre, B.: Standardized precipitation evapotranspiration index (SPEI) revisited: parameter fitting, evapotranspiration models, tools, datasets and drought monitoring, International journal of climatology, 34, 3001–3023, https://doi.org/10.1002/joc.3887, 2014.

Bellaubi, F. and Boehm, F.: Management practices and corruption risks in water service delivery in Kenya and Ghana, Water Policy, 20, 388–409, https://doi.org/10.2166/wp.2018.017, 2018.

Blauhut, V., Gudmundsson, L., and Stahl, K.: Towards pan-European drought risk maps: quantifying the link between drought indices and reported drought impacts, Environmental Research Letters, 10, 014 008, https://doi.org/10.1088/1748-9326/10/1/014008, 2015.

Breiman, L.: Random forests, Machine learning, 45, 5–32, https://doi.org/10.1023/A:1010933404324, 2001.

Cattani, E., Ferguglia, O., Merino, A., and Levizzani, V.: Precipitation Products' Inter–Comparison over East and Southern Africa 1983–2017, Remote Sensing, 13, 4419, https://doi.org/10.3390/rs13214419, 2021.

Change, I. C.: Synthesis Report. Contribution of working groups I, II and III to the fifth assessment report of the intergovernmental panel on climate change, 151, 2014.

Chung, N. C., Miasojedow, B., Startek, M., and Gambin, A.: Jaccard/Tanimoto similarity test and estimation methods for biological presence-absence data, BMC bioinformatics, 20, 1–11, https://doi.org/10.1186/s12859-019-3118-5, 2019.

Dai, M., Huang, S., Huang, Q., Leng, G., Guo, Y., Wang, L., Fang, W., Li, P., and Zheng, X.: Assessing agricultural drought risk and its dynamic evolution characteristics, Agricultural Water Management, 231, 106 003, https://doi.org/10.1016/j.agwat.2020.106003, 2020.

Dee, D. P., Uppala, S. M., Simmons, A. J., Berrisford, P., Poli, P., Kobayashi, S., Andrae, U., Balmaseda, M., Balsamo, G., Bauer, d. P., et al.: The ERA-Interim reanalysis: Configuration and performance of the data assimilation system, Quarterly Journal of the royal meteorological society, 137, 553–597, https://doi.org/10.1002/qj.828, 2011.

EDC: Welcome to the EDII and EDR database, https://www.geo.uio.no/edc/droughtdb/, accessed: 2022-04-29, 2013.

Elreedy, D. and Atiya, A. F.: A comprehensive analysis of synthetic minority oversampling technique (SMOTE) for handling class imbalance, Information Sciences, 505, 32–64, https://doi.org/10.1016/j.ins.2019.07.070, 2019.

Erian, W., Pulwarty, R., Vogt, J., AbuZeid, K., Bert, F., Bruntrup, M., El-Askary, H., de Estrada, M., Gaupp, F., Grundy, M., et al.: GAR Special Report on Drought 2021, 2021.

Essen, C. and Akpan, G.: Analysis of difficulty and point-biserial correlation indices of 2014 Akwa Ibom State Mock Multiple Choices Mathematics Test, International Journal of Education and Evaluation, 4, 1–11, 2018.

Falkenmark, M., Lundqvist, J., and Widstrand, C.: Macro-scale water scarcity requires micro-scale approaches: Aspects of vulnerability in semi-arid development, in: Natural resources forum, vol. 13, pp. 258–267, Wiley Online Library, https://doi.org/10.1111/j.1477-8947.1989.tb00348.x, 1989.

FEWS NET: Kenya food security brief. United States agency for international development (UASID) famine early warning systems network (FEWS NET), https://fews.net/sites/default/files/documents/reports/Kenya_Food%20Security_In_Brief_2013_final_0.pdf, accessed: 2022-17-05, 2013.

FEWS NET: Kenya Food Security Outlook, https://fews.net/sites/default/files/documents/reports/KE%20FSO%20Feb%20-%20Sep%202017_Final.pdf, accessed: 2022-17-05, 2017.

Gudmundsson, L., Rego, F. C., Rocha, M., and Seneviratne, S. I.: Predicting above normal wildfire activity in southern Europe as a function of meteorological drought, Environmental Research Letters, 9, 084 008, https://doi.org/10.1088/1748-9326/9/8/084008, 2014.

Guha-Sapir, D., Below, R., and Hoyois, P.: EM-DAT: the CRED/OFDA international disaster database, 2016.

Hall, J. W. and Leng, G.: Can we calculate drought risk… and do we need to?, Wiley Interdisciplinary Reviews: Water, 6, e1349, https://doi.org/10.1002/wat2.1349, 2019.

Hanley, J. A. and McNeil, B. J.: The meaning and use of the area under a receiver operating characteristic (ROC) curve., Radiology, 143, 29–36, https://doi.org/10.1148/radiology.143.1.7063747, 1982.

Harrigan, S., Zsoter, E., Alfieri, L., Prudhomme, C., Salamon, P., Wetterhall, F., Barnard, C., Cloke, H., and Pappenberger, F.: GloFAS-ERA5 operational global river discharge reanalysis 1979–present, Earth System Science Data, 12, 2043–2060, https://doi.org/10.5194/essd-12-2043-2020, 2020.

Heinrich, D. and Bailey, M.: Forecast-based Financing and Early Action for Drought–Guidance Notes for the Red Cross Red Crescent, 2020.

760 Hersbach, H., Bell, B., Berrisford, P., Hirahara, S., Horányi, A., Muñoz-Sabater, J., Nicolas, J., Peubey, C., Radu, R., Schepers, D., et al.: The ERA5 global reanalysis, Quarterly Journal of the Royal Meteorological Society, 146, 1999–2049, https://doi.org/10.1002/qj.3803, 2020.

Hirpa, F. A., Salamon, P., Beck, H. E., Lorini, V., Alfieri, L., Zsoter, E., and Dadson, S. J.: Calibration of the Global Flood Awareness System (GloFAS) using daily streamflow data, Journal of Hydrology, 566, 595–606, https://doi.org/10.1016/j.jhydrol.2018.09.052, 2018.

Jaccard, P.: The distribution of the flora in the alpine zone. 1, New phytologist, 11, 37–50, https://doi.org/10.1111/j.1469-765 8137.1912.tb05611.x, 1912.

Javadinejad, S., Hannah, D., Ostad-Ali-Askari, K., Krause, S., Zalewski, M., and Boogaard, F.: The impact of future climate change and human activities on hydro-climatological drought, analysis and projections: using CMIP5 climate model simulations, Water Conservation Science and Engineering, 4, 71–88, https://doi.org/10.1007/s41101-019-00069-2, 2019.

Jenkins, M.: The impact of corruption on access to safe water and sanitation for people living in poverty, Anticorruption Resource Center, 770 2017.

Kamruzzaman, M., Almazroui, M., Salam, M., Mondol, M. A. H., Rahman, M., Deb, L., Kundu, P. K., Zaman, M., Uz, A., Islam, A. R. M., et al.: Spatiotemporal drought analysis in Bangladesh using the standardized precipitation index (SPI) and standardized precipitation evapotranspiration index (SPEI), Scientific Reports, 12, 1–17, https://doi.org/10.1038/s41598-022-24146-0, 2022.

Kchouk, S., Melsen, L. A., Walker, D. W., and Van Oel, P. R.: A geography of drought indices: mismatch between indicators of drought and 775 its impacts on water and food securities, Natural Hazards and Earth System Sciences, 22, 323–344, https://doi.org/10.5194/nhess-22-323-2022, 2022.

Kenya: Kenya National Adaptation Plan: 2015–2030, 2016.

Kew, S. F., Philip, S. Y., Hauser, M., Hobbins, M., Wanders, N., Van Oldenborgh, G. J., Van Der Wiel, K., Veldkamp, T. I., Kimutai, J., Funk, C., et al.: Impact of precipitation and increasing temperatures on drought trends in eastern Africa, Earth System Dynamics, 12, 17–35, 780 https://doi.org/10.5194/esd-12-17-2021, 2021.

Kimwatu, D. M., Mundia, C. N., and Makokha, G. O.: Developing a new socio-economic drought index for monitoring drought proliferation: a case study of Upper Ewaso Ngiro River Basin in Kenya, Environmental Monitoring and Assessment, 193, 1–22, https://doi.org/10.1007/s10661-021-08989-0, 2021.

Klisch, A. and Atzberger, C.: Operational drought monitoring in Kenya using MODIS NDVI time series, Remote Sensing, 8, 267, 785 https://doi.org/10.3390/rs8040267, 2016.

Kuhn, M.: Building predictive models in R using the caret package, Journal of statistical software, 28, 1–26, https://doi.org/10.18637/jss.v028.i05, 2008.

Lehner, B., Liermann, C. R., Revenga, C., Vörösmarty, C., Fekete, B., Crouzet, P., Döll, P., Endejan, M., Frenken, K., Magome, J., et al.: High-resolution mapping of the world's reservoirs and dams for sustainable river-flow management, Frontiers in Ecology and the Environment, 790 9, 494–502, https://doi.org/10.1890/100125, 2011.

Liaw, A., Wiener, M., et al.: Classification and regression by randomForest, R news, 2, 18–22, 2002.

Liu, Y. Y., De Jeu, R. A., McCabe, M. F., Evans, J. P., and Van Dijk, A. I.: Global long-term passive microwave satellite-based retrievals of vegetation optical depth, Geophysical Research Letters, 38, https://doi.org/10.1029/2011GL048684, 2011.

Ma, M., Lv, J., Su, Z., Hannaford, J., Sun, H., Qu, Y., Xing, Z., Barker, L., and Wang, Y.: Linking drought indices to impacts in the Liaoning Province of China, Proceedings of the International Association of Hydrological Sciences, 383, 267–272, https://doi.org/10.5194/piahs-383-267-2020, 2020.

Maidment, R. I., Grimes, D., Allan, R. P., Tarnavsky, E., Stringer, M., Hewison, T., Roebeling, R., and Black, E.: The 30 year TAM-SAT African rainfall climatology and time series (TARCAT) data set, Journal of Geophysical Research: Atmospheres, 119, 10–619, https://doi.org/10.1002/2014JD021927, 2014.

Majani, B. S., Malamud, B. D., and Millington, J.: Use of blended evidence sources to build a history of flooding impact and an impact severity scale: A case study of Nairobi, Kenya, Tech. rep., Copernicus Meetings, https://doi.org/10.5194/egusphere-egu22-12012, 2022.

Maliva, R. and Missimer, T.: Arid lands water evaluation and management, Springer Science & Business Media, 2012.

Martens, B., Miralles, D. G., Lievens, H., Van Der Schalie, R., De Jeu, R. A., Fernández-Prieto, D., Beck, H. E., Dorigo, W. A., and Verhoest, N. E.: GLEAM v3: Satellite-based land evaporation and root-zone soil moisture, Geoscientific Model Development, 10, 1903–1925, https://doi.org/10.5194/gmd-10-1903-2017, 2017.

McKee, T. B., Doesken, J., and Kleist, J.: Analysis of Standardized Precipitation Index (SPI) data for drought assessment, Water, 26, 1–72, 1993.

McNally, A., Verdin, K., Harrison, L., Getirana, A., Jacob, J., Shukla, S., Arsenault, K., Peters-Lidard, C., and Verdin, J. P.: Acute water-scarcity monitoring for Africa, Water, 11, 1968, https://doi.org/10.3390/w11101968, 2019.

Miralles, D. G., Holmes, T., De Jeu, R., Gash, J., Meesters, A., and Dolman, A.: Global land-surface evaporation estimated from satellite-based observations, Hydrology and Earth System Sciences, 15, 453–469, https://doi.org/10.5194/hess-15-453-2011, 2011.

Mishra, A. K. and Singh, V. P.: A review of drought concepts, Journal of hydrology, 391, 202–216, https://doi.org/10.1016/j.jhydrol.2010.07.012, 2010.

Mude, A. G., Ouma, R., Steeg, J. v. d., Kaiuki, J., Opiyo, D., and Tipilda, A.: Kenya adaptation to climate change in the arid lands: Anticipating, adapting to and coping with climate risks in Kenya-Operational recommendations for KACCAL, ILRI Research Report, 2007.

Mulwa, F., Li, Z., and Fangninou, F. F.: Water Scarcity in Kenya: Current Status, Challenges and Future Solutions, Open Access Library Journal, 8, 1–15, https://doi.org/10.4236/oalib.1107096, 2021.

Mutsotso, R. B., Sichangi, A. W., and Makokha, G. O.: Spatio-temporal drought characterization in Kenya from 1987 to 2016, https://doi.org/10.4236/ars.2018.72009, 2018.

Mwangi, E., Taylor, O., Todd, M. C., Visman, E., Kniveton, D., Kilavi, M., Ndegwa, W., Otieno, G., Waruru, S., Mwangi, J., et al.: Mainstreaming forecast based action into national disaster risk management systems: experience from drought risk management in Kenya, Climate and Development, 14, 741–756, https://doi.org/10.1080/17565529.2021.1984194, 2022.

Nalbantis, I.: Evaluation of a hydrological drought index, European Water, 23, 67–77, 2008.

NDMC: Drought Impact Reporter, https://droughtreporter.unl.edu/map/, accessed: 2022-04-29, 2005.

Nicolai-Shaw, N., Zscheischler, J., Hirschi, M., Gudmundsson, L., and Seneviratne, S. I.: A drought event composite analysis using satellite remote-sensing based soil moisture, Remote Sensing of Environment, 203, 216–225, https://doi.org/10.1016/j.rse.2017.06.014, 2017.

Niwattanakul, S., Singthongchai, J., Naenudorn, E., and Wanapu, S.: Using of Jaccard coefficient for keywords similarity, in: Proceedings of the international multiconference of engineers and computer scientists, vol. 1, pp. 380–384, 2013.

Njarui, D., Gatheru, M., and Ghimire, S. R.: Brachiaria grass for climate resilient and sustainable livestock production in Kenya, African Handbook of Climate Change Adaptation, pp. 1–22, https://doi.org/10.1007/978-3-030-42091-8_146-1, 2020.

Nyberg, Y., Jonsson, M., Laszlo Ambjörnsson, E., Wetterlind, J., and Öborn, I.: Smallholders' awareness of adaptation and coping measures to deal with rainfall variability in Western Kenya, Agroecology and Sustainable Food Systems, 44, 1280–1308, https://doi.org/10.1080/21683565.2020.1782305, 2020.

O'Connor, P., Murphy, C., Matthews, T., and Wilby, R. L.: Relating drought indices to impacts reported in newspaper articles, International Journal of Climatology, https://doi.org/10.1002/joc.7946, 2022.

Ondiko, J. H. and Karanja, A. M.: Spatial and Temporal Occurrence and Effects of Droughts on Crop Yields in Kenya, Open Access Library Journal, 8, 1–13, https://doi.org/10.4236/oalib.1107354, 2021.

Opiyo, F., Wasonga, O., Nyangito, M., Schilling, J., and Munang, R.: Drought adaptation and coping strategies among the Turkana pastoralists of northern Kenya, International Journal of Disaster Risk Science, 6, 295–309, https://doi.org/10.1007/s13753-015-0063-4, 2015.

Parry, J.-E.: Review of current and planned adaptation action in Kenya, 2016.

Parsons, D. J., Rey, D., Tanguy, M., and Holman, I. P.: Regional variations in the link between drought indices and reported agricultural impacts of drought, Agricultural systems, 173, 119–129, https://doi.org/10.1016/j.agsy.2019.02.015, 2019.

Peng, J., Dadson, S., Hirpa, F., Dyer, E., Lees, T., Miralles, D. G., Vicente-Serrano, S. M., and Funk, C.: A pan-African high-resolution drought index dataset, Earth System Science Data, 12, 753–769, https://doi.org/10.5194/essd-12-753-2020, 2020.

Phillip, M. J.: Combating Water Scarcity in Southern Africa: Case Studies from Namibia, Springer, https://doi.org/10.1007/978-94-007-7097-3, 2013.

Priestley, C. H. B. and Taylor, R. J.: On the assessment of surface heat flux and evaporation using large-scale parameters, Monthly weather review, 100, 81–92, https://doi.org/10.1175/1520-0493(1972)100<0081:OTAOSH>2.3.CO;2, 1972.

Quandt, A.: Coping with drought: narratives from smallholder farmers in semi-arid Kenya, International Journal of Disaster Risk Reduction, 57, 102 168, https://doi.org/10.1016/j.ijdrr.2021.102168, 2021.

Savelli, E., Rusca, M., Cloke, H., and Di Baldassarre, G.: Don't blame the rain: Social power and the 2015–2017 drought in Cape Town, Journal of Hydrology, 594, 125 953, https://doi.org/10.1016/j.jhydrol.2020.125953, 2021.

Savelli, E., Rusca, M., Cloke, H., and Di Baldassarre, G.: Drought and society: Scientific progress, blind spots, and future prospects, Wiley Interdisciplinary Reviews: Climate Change, p. e761, https://doi.org/10.1002/wcc.761, 2022.

Seneviratne, S., Nicholls, N., Easterling, D., Goodess, C., Kanae, S., Kossin, J., Luo, Y., Marengo, J., McInnes, K., Rahimi, M., et al.: Changes in climate extremes and their impacts on the natural physical environment, 2012.

Seneviratne, S. I., Zhang, X., Adnan, M., Badi, W., Dereczynski, C., Di Luca, A., Vicente-Serrano, S. M., Wehner, M., and Zhou, B.: 11 Chapter 11: Weather and climate extreme events in a changing climate, 2021.

Stagge, J. H., Kohn, I., Tallaksen, L. M., and Stahl, K.: Modeling drought impact occurrence based on meteorological drought indices in Europe, Journal of Hydrology, 530, 37–50, https://doi.org/10.1016/j.jhydrol.2015.09.039, 2015.

Stahl, K., Kohn, I., Blauhut, V., Urquijo, J., De Stefano, L., Acácio, V., Dias, S., Stagge, J. H., Tallaksen, L. M., Kampragou, E., et al.: Impacts of European drought events: insights from an international database of text-based reports, Natural Hazards and Earth System Sciences, 16, 801–819, https://doi.org/10.5194/nhess-16-801-2016, 2016.

Sutanto, S. J. and Van Lanen, H. A.: Catchment memory explains hydrological drought forecast performance, Scientific reports, 12, 1–11, https://doi.org/10.1038/s41598-022-06553-5, 2022.

Tarnavsky, E., Grimes, D., Maidment, R., Black, E., Allan, R. P., Stringer, M., Chadwick, R., and Kayitakire, F.: Extension of the TAMSAT satellite-based rainfall monitoring over Africa and from 1983 to present, Journal of Applied Meteorology and Climatology, 53, 2805–2822, https://doi.org/10.1175/JAMC-D-14-0016.1, 2014.

The World Bank: Population, data retrieved from World Development Indicators, https://data.worldbank.org/indicator/SP.POP.TOTL, 2020.

870 Thomas, E., Jordan, E., Linden, K., Mogesse, B., Hailu, T., Jirma, H., Thomson, P., Koehler, J., and Collins, G.: Reducing drought emergencies in the Horn of Africa, Science of the Total Environment, 727, 138 772, https://doi.org/10.1016/j.scitotenv.2020.138772, 2020.

UNESCO: Map of the world distribution of arid regions: Map at scale 1:25,000,000 with explanatory note., MAB Technical Notes 7, UNESCO, Paris, 1979.

Van Der Knijff, J., Younis, J., and De Roo, A.: LISFLOOD: a GIS-based distributed model for river basin scale water balance and flood

875 simulation, International Journal of Geographical Information Science, 24, 189–212, https://doi.org/10.1080/13658810802549154, 2010.

Van Dijk, A. I., Beck, H. E., Crosbie, R. S., de Jeu, R. A., Liu, Y. Y., Podger, G. M., Timbal, B., and Viney, N. R.: The Millennium Drought in southeast Australia (2001–2009): Natural and human causes and implications for water resources, ecosystems, economy, and society, Water Resources Research, 49, 1040–1057, https://doi.org/10.1002/wrcr.20123, 2013.

Van Loon, A. F.: Hydrological drought explained, Wiley Interdisciplinary Reviews: Water, 2, 359–392, https://doi.org/10.1002/wat2.1085,

880 2015.

Van Loon, A. F. and Van Lanen, H. A.: Making the distinction between water scarcity and drought using an observation-modeling framework, Water Resources Research, 49, 1483–1502, https://doi.org/10.1002/wrcr.20147, 2013.

Van Loon, A. F., Gleeson, T., Clark, J., Van Dijk, A. I., Stahl, K., Hannaford, J., Di Baldassarre, G., Teuling, A. J., Tallaksen, L. M., Uijlenhoet, R., et al.: Drought in the Anthropocene, Nature Geoscience, 9, 89–91, https://doi.org/10.1038/ngeo2646, 2016a.

885 Van Loon, A. F., Stahl, K., Di Baldassarre, G., Clark, J., Rangecroft, S., Wanders, N., Gleeson, T., Van Dijk, A. I., Tallaksen, L. M., Hannaford, J., et al.: Drought in a human-modified world: reframing drought definitions, understanding, and analysis approaches, Hydrology and Earth System Sciences, 20, 3631–3650, https://doi.org/10.5194/hess-20-3631-2016, 2016b.

Vicente-Serrano, S. M., Beguería, S., and López-Moreno, J. I.: A multiscalar drought index sensitive to global warming: the standardized precipitation evapotranspiration index, Journal of climate, 23, 1696–1718, https://doi.org/10.1175/2009JCLI2909.1, 2010.

890 Wamucii, C. N., van Oel, P. R., Ligtenberg, A., Gathenya, J. M., and Teuling, A. J.: Land use and climate change effects on water yield from East African forested water towers, Hydrology and Earth System Sciences, 25, 5641–5665, https://doi.org/10.5194/hess-25-5641-2021, 2021.

Wanders, N., Van Loon, A. F., and Van Lanen, H. A.: Frequently used drought indices reflect different drought conditions on global scale, Hydrology and Earth System Sciences Discussions, pp. 1–16, https://doi.org/10.5194/hess-2017-512, 2017.

895 Wang, R., Li, L., Gentine, P., Zhang, Y., Chen, J., Chen, X., Chen, L., Ning, L., Yuan, L., and Lü, G.: Recent increase in the observation-derived land evapotranspiration due to global warming, Environmental Research Letters, 17, 024 020, https://doi.org/10.1088/1748-9326/ac4291, 2022.

Wang, W., Ertsen, M. W., Svoboda, M. D., and Hafeez, M.: Propagation of drought: from meteorological drought to agricultural and hydrological drought, https://doi.org/10.1155/2016/6547209, 2016.

900 Wang, Y., Lv, J., Hannaford, J., Wang, Y., Sun, H., Barker, L. J., Ma, M., Su, Z., and Eastman, M.: Linking drought indices to impacts to support drought risk assessment in Liaoning province, China, Natural Hazards and Earth System Sciences, 20, 889–906, https://doi.org/10.5194/nhess-20-889-2020, 2020.

weADAPT: Enhancing resiliency to drought in Kenya's arid and semi-arid lands, https://www.weadapt.org/, 2023.

WFP, V.: Food consumption analysis: calculation and use of the food consumption score in food security analysis, WFP: Rome, Italy, 2008.

905 Wilhite, D. A., Svoboda, M. D., and Hayes, M. J.: Understanding the complex impacts of drought: A key to enhancing drought mitigation and preparedness, Water resources management, 21, 763–774, https://doi.org/10.1007/s11269-006-9076-5, 2007.

WMO: WMO Guidelines on Multi-hazard Impact-based Forecast and Warning Services, wMO-No. 1150, 2015.

Xu, H.-j., Wang, X.-p., Zhao, C.-y., Shan, S.-y., and Guo, J.: Seasonal and aridity influences on the relationships between drought indices and hydrological variables over China, Weather and Climate Extremes, 34, 100 393, https://doi.org/10.1016/j.wace.2021.100393, 2021.

910   Xu, Y., Zhang, X., Wang, X., Hao, Z., Singh, V. P., and Hao, F.: Propagation from meteorological drought to hydrological drought under the impact of human activities: A case study in northern China, Journal of Hydrology, 579, 124 147, https://doi.org/10.1016/j.jhydrol.2019.124147, 2019.

Yihdego, Y., Vaheddoost, B., and Al-Weshah, R. A.: Drought indices and indicators revisited, Arabian Journal of Geosciences, 12, 1–12, https://doi.org/10.1007/s12517-019-4237-z, 2019.

915   Zhou, Y., Zhou, P., Jin, J., Wu, C., Cui, Y., Zhang, Y., and Tong, F.: Drought identification based on Palmer drought severity index and return period analysis of drought characteristics in Huaibei Plain China, Environmental Research, 212, 113 163, https://doi.org/10.1016/j.envres.2022.113163, 2022.